LBL-34081
UC-331

Lawrence Berkeley Laboratory

UNIVERSITY OF CALIFORNIA

ENERGY & ENVIRONMENT DIVISION

Exploratory Technology Research Program for Electrochemical Energy Storage

Annual Report for 1992

K. Kinoshita, Editor

October 1993

ENERGY & ENVIRONMENT DIVISION

REFERENCE COPY
Does Not
Circulate
Bldg. 50 Library.
LBL-34081
Copy 1

Prepared for the U.S. Department of Energy under Contract Number DE-AC03-76SF00098

DISCLAIMER

This document was prepared as an account of work sponsored by the United States Government. While this document is believed to contain correct information, neither the United States Government nor any agency thereof, nor the Regents of the University of California, nor any of their employees, makes any warranty, express or implied, or assumes any legal responsibility for the accuracy, completeness, or usefulness of any information, apparatus, product, or process disclosed, or represents that its use would not infringe privately owned rights. Reference herein to any specific commercial product, process, or service by its trade name, trademark, manufacturer, or otherwise, does not necessarily constitute or imply its endorsement, recommendation, or favoring by the United States Government or any agency thereof, or the Regents of the University of California. The views and opinions of authors expressed herein do not necessarily state or reflect those of the United States Government or any agency thereof or the Regents of the University of California.

LBL-34081

EXPLORATORY TECHNOLOGY RESEARCH PROGRAM FOR ELECTROCHEMICAL ENERGY STORAGE

ANNUAL REPORT FOR 1992

Energy & Environment Division
Lawrence Berkeley Laboratory
University of California
Berkeley, California 94720

Edited by Kim Kinoshita, Technical Manager

October 1993

This work was supported by the Assistant Secretary for Energy Efficiency and Renewable Energy, Office of Transportation Technologies, Electric & Hybrid Propulsion Division of the U.S. Department of Energy under Contract No. DE-AC03-76SF00098.

CONTENTS

EXECUTIVE SUMMARY v
I. INTRODUCTION 1
II. EXPLORATORY RESEARCH
A. ADVANCED ZINC/NICKEL OXIDE CELLS
Zn/NiOOH Cell Studies 2
Applied Research on Secondary Zn/NiOOH Cell Technology 3
B. SOLID-STATE SODIUM/POLYMER CELLS
Electrochemical Properties of Solid-State Sodium/Polymer Cells 4
III. APPLIED SCIENCE RESEARCH
A. ELECTRODE CHARACTERIZATION
Surface Morphology of Metals in Electrodeposition 8
Battery Materials: Structure and Characterization 9
B. COMPONENTS FOR HIGH-TEMPERATURE CELLS
High-Temperature Cell Research 10
C. CORROSION PROCESSES IN HIGH-SPECIFIC-ENERGY CELLS
Corrosion-Resistant Coatings for High-Temperature High-Sulfur-Activity Batteries 10
Improved Container Electrode Coating for Na/S Battery Systems 11
Corrosion, Passivity, and Breakdown of Alloys Used in High-Energy Batteries 12
D. COMPONENTS FOR AMBIENT-TEMPERATURE NONAQUEOUS CELLS
Spectroscopic Studies of the Passive Film on Alkali and Alkaline Earth Metals in Nonaqueous Solvents 13
In Situ Spectroscopic Applications to the Study of Rechargeable Lithium Batteries 15
E. CROSS-CUTTING RESEARCH
Analysis and Simulation of Electrochemical Systems 17
Electrode Surface Layers 19
Electrode Kinetics and Electrocatalysis of Methanol Electrooxidation 20
Effect of Electrocatalyst and Electrolyte Composition on Methanol/Air Fuel Cell Performance 21
IV. AIR SYSTEMS RESEARCH
A. METAL/AIR CELL RESEARCH
Electrocatalysts for Oxygen Electrodes 23
Novel Concepts for Oxygen Electrodes in Secondary Metal/Air Battery 26
Transport in Zinc-Air Cells and Mathematical Modeling 26
Development of Electrically Rechargeable Zinc-Air Cells 27
B. FUEL CELL RESEARCH
Fuel Cells for Renewable Applications 28
Electrocatalysis of Fuel Cells Reactions 33

EXECUTIVE SUMMARY

The U.S. Department of Energy's Office of Propulsion Systems provides support for an Electrochemical Energy Storage Program, that includes research and development (R&D) on advanced rechargeable batteries and fuel cells. A major goal of this program is to develop electrochemical power sources suitable for application in electric vehicles (EVs). The program centers on advanced systems that offer the potential for high performance and low life-cycle costs, both of which are necessary to permit significant penetration into commercial markets.

The DOE Electrochemical Energy Storage Program is divided into two projects: the Electric Vehicle Advanced Battery Systems (EVABS) Development Program and the Exploratory Technology Research (ETR) Program. The EVABS Program management responsibility has been assigned to Sandia National Laboratory (SNL), and the Lawrence Berkeley Laboratory* (LBL) is responsible for management of the ETR Program. The EVABS and ETR Programs include an integrated matrix of R&D efforts designed to advance progress on selected candidate electrochemical systems. The United States Advanced Battery Consortium (USABC), a tripartite undertaking between DOE, the U.S. automobile manufacturers and the Electric Power Research Institute (EPRI), was formed in 1991 to accelerate the development of advanced batteries for consumer EVs. The role of the ETR Program is to perform supporting research on the advanced battery systems under development by the USABC and EVABS Program, and to evaluate new systems with potentially superior performance, durability and/or cost characteristics. The specific goal of the ETR Program is to identify the most promising electrochemical technologies and transfer them to the USABC, the battery industry and/or the EVABS Program for further development and scale-up. This report summarizes the research, financial and management activities relevant to the ETR Program in CY 1992. This is a continuing program, and reports for prior years have been published; they are listed at the end of this Executive Summary.

The general R&D areas addressed by the program include identification of new electrochemical couples for advanced batteries, determination of technical feasibility of the new couples, improvements in battery components and materials, establishment of engineering principles applicable to electrochemical energy storage and conversion, and the development of air-system (fuel cell, metal/air) technology for transportation applications. Major emphasis is given to applied research which will lead to superior performance and lower life-cycle costs.

---

* Participants in the ETR Program include the following LBL scientists: E. Cairns, K. Kinoshita and F. McLarnon of the Energy and Environment Division; and L. DeJonghe, J. Evans, J. Newman, P. Ross and C. Tobias of the Materials Sciences Division.

The ETR Program is divided into three major program elements: Exploratory Research, Applied Science Research, and Air Systems Research. Highlights of each program element are summarized according to the appropriate battery system or electrochemical research area.

EXPLORATORY RESEARCH

The objectives of this program element are to identify, evaluate and initiate development of new electrochemical couples with the potential to meet or exceed advanced battery and electrochemical performance goals. Research was conducted on new versions of the **Zn/NiOOH cell** and a novel **Na/polymer cell**. Each of these cells is considered to be an attractive candidate for EV applications, and should provide high performance at ambient or near-ambient temperatures. A Zn/NiOOH battery would exhibit higher performance and lower costs, compared to the MH/NiOOH battery; and a Na/polymer battery would lower cost, compared to a Li/polymer battery.

- LBL has observed that the Zn/KOH/NiOOH cell capacity retention and NiOOH electrode coulombic efficiencies are superior in cells containing NiOOH electrodes loaded at 1.3 g/cm^3 void space, compared to cells containing NiOOH electrodes loaded at 1.6 g/cm^3 void space.
- A subcontract was awarded to the Advanced Energy Systems Division of Acme Electric Corporation on the basis of a Request-for-Proposals to extend the development of Zn/NiOOH cell technology. The objectives of this project are to evaluate the LBL electrolyte composition for extending the cycle life of Zn/NiOOH cells and to develop Zn/NiOOH battery technology for EV applications. Formation cycles of cells containing sintered Ni positive/plastic-bonded Zn negative or fiber-bonded Ni positive/plastic-bonded Zn negative showed that good cell capacities can be obtained, but indicate that some technical issues must be resolved to achieve the state-of-the-art performance obtained at LBL.
- Cycle testing of Na/PEO/$Na_{0.6}CoO_2$ cells is underway at LBL. Over 100 cycles were obtained at 0.5 mA/cm^2 to 50% capacity and up to 200 cycles at somewhat lower depths of discharge.

APPLIED SCIENCE RESEARCH

The objectives of this program element are to provide and establish scientific and engineering principles applicable to batteries and electrochemical systems; and to identify, characterize and improve materials and components for use in batteries and electrochemical systems. Projects

in this element provide research that supports a wide range of battery systems — alkaline, metal/air, flow, solid-electrolyte and nonaqueous. Other cross-cutting research efforts are directed at improving the understanding of electrochemical engineering principles, minimizing corrosion of battery components, analyzing the surfaces of electrodes, and electrocatalysis. **Electrode Characterization** studies are an important research element for the successful development of rechargeable electrodes for advanced secondary batteries. Efforts are underway to determine the role of surface morphology on mass transport which may affect the morphology of electrodeposits. Advanced spectroscopic techniques are utilized to investigate the chemical state of electrode materials during charge/discharge cycling.

- LBL is extending the study on the effect of protrusions on mass transport to electrodeposited surface layers, and the coalescence of electrolytic gas bubbles which may affect the morphology of electrodeposits. A mathematical model has been developed that uses the Boundary Integral Element Method (BIEM) to understand the hydrodynamics of flow over protrusions. Electrochemical cells to study this phenomena and to observe the coalescence of electrolytic gas bubbles were designed and fabricated.
- Brookhaven National Laboratory (BNL) has used extended X-ray absorption fine structure (EXAFS) and X-ray absorption near-edge spectroscopy (XANES) to study manganese oxides compounds, Bi-doped manganese oxide and $Li_x MnO_2$. EXAFS data were obtained at both the Mn K edge and the Bi L_3 edge for Bi-doped manganese oxide that was discharged in 9 M KOH. At the end of the one-electron discharge the manganese oxide is highly disordered, while on completion of the two-electron discharge, the product reverts back to an ordered phase.

Improved Components for Alkali/Sulfur Cells, such as superior alternatives to the high-temperature sulfur-polysulfide electrode for Na/S cells, are under investigation.

- LBL demonstrated that the performance of sulfur electrodes is markedly improved by the addition of phosphorus. The study showed that the best performance in Na/S cells was obtained with a P/S ratio of 0.143 in the range 0.143 to 1.17. Equilibrium electromotive force (EMF) measurements showed that at least three three-phase regions were present in the Na-P-S ternary system at 350 and 400°C. A Na/S_xP_y battery would exhibit ~11% higher specific energy than a comparable Na/S battery.

Corrosion Processes in High-Specific-Energy Cells are under investigation, and the aim is to develop low-cost container and current-collector materials for use in nonaqueous, alkali/sulfur and molten-salt cells.

- Illinois Institute of Technology (IIT) is evaluating the quality of Mo_2C coatings obtained by plasma-enhanced chemical vapor deposition (CVD). X-ray photoelectron spectroscopy (XPS) analysis indicate that the films deposited on a glass or steel substrate contain a significant fraction of oxygen. The use of hydrogen and methane as a carrier gas is being evaluated to minimize the oxygen activity in the reaction chamber.

- The Environmental Research Institute of Michigan (ERIM) has prepared TiN-coated Al containment materials by sputter-deposition techniques for corrosion testing in molten Na_2S_4 at 350°C. After three weeks in the polysulfide melt a conductive surface film was still present on the sample coated with TiN. Final analyses of the physicochemical properties of the coating have not been completed.

- Johns Hopkins University has extended the studies on the passivation and anodic behavior of iron and 1018 carbon steel in $LiAsF_6$/dimethoxyethane (DME). In a nominally dry $LiAsF_6$/DME solution containing 50-100 ppm H_2O, the dissolution of Fe and the electropolymerization of the DME solvent are believed to play a major role in the repassivation mechanism. In addition, the electropolymerization reaction is dependent on the presence of $LiAsF_6$; no polymerization is observed in its absence or when other salts are present instead.

Components for Ambient-Temperature Nonaqueous Cells, particularly metal/electrolyte combinations that improve the rechargeability of these cells, are under investigation.

- Case Western Reserve University (CWRU) has used *in situ* spectroscopic techniques and thermal analysis to study the Li/organic electrolyte interface. X-ray photoelectron spectroscopy (XPS) studies indicate that the interactions between Li and perdeuterated tetrahydrofuran (TDF) are strong, leading to substantial structural modifications. Thermal desorption studies with TDF revealed that Li can dehydrogenate TDF to form LiD as one of the predominant products. This type of information is needed to develop a Li electrode/electrolyte combination that exhibits reversible behavior.

- CWRU is utilizing *in situ* EXAFS and XANES to investigate electrochemical phenomena in Li/polymer electrolyte and Li/FeS_2 cells. Initial effort has centered on studies of Li/FeS_2 cells that operate at room temperature. During discharge Li is inserted into FeS_2, and the corresponding EXAFS spectra revealed a gradual loss in the fine structure as the amount of Li is increased.

Cross-Cutting Research is carried out to develop mathematical models of electrochemical systems and to address fundamental problems in electrocatalysis and current-density distribution; solutions will lead to improved electrode structures and performance in batteries and fuel cells.

- LBL has developed mathematical models to understand transport and kinetic phenomena occurring in selected electrochemical systems. Models have been developed to predict the behavior of Li/polymer electrolyte/metal oxide cells during charge and discharge. Comparisons were made between cells that contain a Li metal negative and Li-intercalated carbon negative.
- LBL has used ion implantation to modify the properties of Ni electrodes for alkaline batteries and grid materials for lead-acid batteries. Co-implanted Ni electrodes appear to have a higher coulombic storage capacity than comparable electrodes without the addition of Co. On the other hand, Cu implantation has the opposite effect. Implantation of Ti in Pb and Pb-4%Sb grids reduces the corrosion current in 5 M H_2SO_4 by a factor of about 30-fold and 70-fold, respectively.
- LBL has observed that the highest activity for the methanol electrooxidation on Pt-Ru alloys occurs on an alloy with a surface composition of 10 at% Ru. On these alloys, the adsorption of methanol is believed to occur on the three-fold Pt surface sites where the hydrogen of the methanol is oxidized. The remaining CO fragment diffuses to the neighboring Ru where it undergoes oxidation. These studies help point the way to the development of a stable, high-performance direct-methanol fuel cell (DMFC).
- LBL has observed that the performance of dispersed Pt-Ru for the electrooxidation of vaporized methanol in 72 wt% Cs_2 CO_3 reached a maximum at a temperature of 10 to 15°C below the boiling point of the electrolyte. This performance level is the highest ever observed for a DMFC with low catalyst loading.

AIR SYSTEMS RESEARCH

The objectives of this program element are to identify, characterize and improve materials for air electrodes; and to identify, evaluate and initiate development of metal/air battery systems and fuel-cell technology for transportation applications.

Metal/Air Cell Research projects address bifunctional air electrodes, that are needed for electrically rechargeable metal/air (Zn/air, Fe/air) cells; and novel alkaline Zn electrode structures, that could be used in either electrically recharged or mechanically recharged cell configurations.

- CWRU has completed an extensive 8-year (1984-1992) study of oxygen electrocatalysis on various transition-metal macrocyles and oxide catalysts. This effort resulted in a better understanding of O_2 reduction and evolution on these electrocatalysts in acid and alkaline electrolytes. The significant accomplishments of the research are summarized.
- Eltech Research Corporation is investigating the viability of graphitized carbon blacks and metal oxides as electrocatalyst supports in bifunctional air electrodes for electrically rechargeable Zn/air cells. Graphitized carbon blacks of both Monarch 120 and Shawinigan acetylene black appear to be suitable electrocatalyst supports. Electrochemical tests of $NiCo_2O_4$/Monarch 120 in small cells at MATSI achieved over 350 cycles (discharge 4 h at 10 mA/cm^2, charge 8 h at 5 mA/cm^2).
- LBL has operated a Zn/air cell which employed a reticulated Zn electrode structure under natural convection. A small laboratory cell (77 cm^2 air-electrode active area) was operated at 20 mA/cm^2 at an average cell voltage of 0.9 V. Measurements with a laser-Doppler velocimeter showed that the electrolyte velocity under natural convective flow during cell discharge was 0.1 mm/s. This kind of Zn/air cell would be simpler to operate and more reliable than other Zn/air cells with flowing electrolyte.
- LBL evaluated several procedures to prepare $La_{0.6}Ca_{0.4}CoO_3$ which has shown promise as an electrocatalyst in bifunctional air electrodes. The amorphous citrate precursor method yielded fairly pure powders with limited crystallinity and BET surface areas up to 18 m^2/g. A preliminary cycle life of 45 cycles in an electrolyte of 45 wt% KOH and 40 g Zn^{2+}/l was obtained with the electrocatalyst in gas-diffusion electrodes, which may be limited by flooding of the electrode and/or slow degradation of the electrocatalyst.

Fuel Cell Research at Los Alamos National Laboratory (LANL) includes research in several areas of electrochemistry, theoretical studies, fuel-cell testing, fuel processing, and membrane characterization. Major achievements of the fuel-cell program during 1992 are listed below:

- LANL has found that processing membrane-electrode assemblies (MEA) with Nafion membranes that contain tetrabutyl ammonium are more robust than those obtained from the Na^+ and H^+ forms.

- Life tests of up to 4000 h have been achieved by LANL with only a 10% performance loss with membrane/electrode assemblies with thin-layer catalyst layers in polymer electrolyte fuel cells (PEFC) at 80°C.
- A new membrane from DuPont (Nafion 5L) was evaluated by LANL. It showed a protonic conductivity of about 20% higher than that for Nafion 117. Its water uptake was also about a factor of 2 larger than that for Nafion 117, membrane C, and an experimental Dow membrane.
- LANL has clarified the influence of CO_2 on the performance of anodes in PEFCs. The study showed that the reverse shift reaction involving CO_2 and the electrochemical reduction of CO_2 both produce CO which poisons the anode.
- Permeation of CH_3OH through Nafion was studied by LANL in PEFCs. Permeation rates equivalent to 200 mA/cm^2 were determined with 45% CH_3OH in the fuel stream.
- LANL obtained self diffusion coefficients of 1.4×10^{-5} cm^2/s and 2×10^{-5} cm^2/s for H_2O and CH_3OH, respectively, in Nafion using nuclear magnetic resonance (NMR).
- BNL is utilizing X-ray absorption spectroscopy (XAS) to study the correlation between the electronic properties of carbon supported Pt/Cr, Pt/Co and Pt/Ni alloy catalysts and their electrocatalytic activity for oxygen reduction. The results indicate that alloying Pt enhances the performance of the oxygen electrode in a PEFC operating at 95°C and at 5-atm pressure.

MANAGEMENT ACTIVITIES

During 1992, LBL managed 15 subcontracts and conducted a vigorous research program in electrochemical energy storage. LBL staff members attended project review meetings, made site visits to subcontractors, and participated in technical management of various ETR projects. LBL staff members also participated in the following reviews, meetings, and workshops:

- Fuel Cells for Transportation Meeting, Washington, D.C., January 6-7, 1992
- IECEC Planning Meeting, San Diego, CA, January 23-24, 1992
- Zn/Air Review Meeting, Sandia National Laboratories, Albuquerque, NM, February 4, 1992
- USABC Technical Advisory Committee Meeting, EPRI, Palo Alto, CA, February 11, 1992
- Power Sources Manufacturers Association - Battery R&D Committee Meeting, Colorado Springs, CO, February 13-14, 1992

- 203rd American Chemical Society National Meeting, San Francisco, CA, April 5-10, 1992
- 1992 Spring Meeting - Materials Research Society, San Francisco, CA, April 27-May 1, 1992
- EPRI/GRI Fuel Cell Workshop, San Francisco, CA, April 29-30, 1992
- 181st Meeting of the Electrochemical Society, St. Louis, MO, May 17-22, 1992
- Fuel Cells for Transportation Meeting, Santa Fe, NM, June 9-11, 1992
- Workshop on Advanced Battery Technology R&D, Willowbrook, IL, June 16-17, 1992
- 4th Quarterly Progress Review of EPRI Contract for Development of Sealed Bipolar Zn/NiOOH Batteries, Energy Research Corporation, Danbury, CT, July 10, 1992
- 27th Meeting of IECEC, San Diego, CA, August 3-7, 1992
- SNL/DOE Zinc/Air Battery Development Program Kickoff Meeting, Westinghouse Electric Corporation, Pittsburgh, PA, August 21, 1992
- Power Sources Manufacturers' Association Meeting, Tinton Falls, NJ, September 2, 1992
- 43rd Meeting of the ISE, Cordoba, Argentina, September 19-23, 1992
- 182nd Meeting of the Electrochemical Society, Toronto, Canada, October 11-16, 1992
- Supercities Conference, San Francisco, CA, October 27, 1992
- Annual Automotive Technology Development Contractors' Coordination Meeting, Dearborn, MI, November 2-5, 1992
- Final Review of the ERC Nickel-Zinc Battery Development Project with EPRI, Palo Alto, CA, December 4, 1992

ACKNOWLEDGMENT

This work was supported by the Assistant Secretary for Energy Efficiency and Renewable Energy, Office of Propulsion Systems, Energy & Hybrid Propulsion Division of the U.S. Department of Energy under Contract No. DE-AC03-76SF00098. The support from DOE and the contributions by the participants in the ETR Program are acknowledged. The assistance of Ms. Susan Lauer for coordinating the publication of this report and Mr. Garth Burns for providing the financial data are gratefully acknowledged.

ANNUAL REPORTS

1. "Technology Base Research Project for Electrochemical Energy Storage - Annual Report for 1991," LBL-32212 (June 1992).
2. "Technology Base Research Project for Electrochemical Energy Storage - Annual Report for 1990," LBL-30846 (June 1991).
3. "Technology Base Research Project for Electrochemical Energy Storage - Annual Report for 1989," LBL-29155 (May 1990).
4. "Technology Base Research Project for Electrochemical Energy Storage - Annual Report for 1988," LBL-27037 (May 1989).
5. "Technology Base Research Project for Electrochemical Energy Storage - Annual Report for 1987," LBL-25507 (July 1988).
6. "Technology Base Research Project for Electrochemical Energy Storage - Annual Report for 1986," LBL-23495 (July 1987).
7. "Technology Base Research Project for Electrochemical Energy Storage - Annual Report for 1985," LBL-21342 (July 1986).
8. "Technology Base Research Project for Electrochemical Energy Storage - Annual Report for 1984," LBL-19545 (May 1985).
9. "Annual Report for 1983 - Technology Base Research Project for Electrochemical Energy Storage," LBL-17742 (May 1984).
10. "Technology Base Research Project for Electrochemical Energy Storage - Annual Report for 1982" LBL-15992 (May 1983).
11. Technology Base Research Project for Electrochemical Energy Storage - Report for 1981," LBL-14305 (June 1982).
12. "Applied Battery and Electrochemical Research Program Report for 1981," LBL-14304 (June 1982).
13. "Applied Battery and Electrochemical Research Program Report for Fiscal Year 1980," LBL-12514 (April 1981).

LIST OF ACRONYMS

AES	Auger electron spectroscopy
AFM	atomic force microscopy
BIEM	Boundary Integral Element Method
BNL	Brookhaven National Laboratory
CMD	chemical manganese dioxide
CVD	chemical vapor deposition
CWRU	Case Western Reserve University
DME	dimethoxyethane
DMPEFC	direct methanol polymer electrolyte fuel cell
DOE	Department of Energy
EMD	electrolytic manganese dioxide
EMF	equilibrium electromotive force
EPRI	Electric Power Research Institute
ERIM	Environmental Research Institute of Michigan
ETR	Exploratory Technology Research
EV	electric vehicle
EVABS	Electric Vehicle Advanced Battery Systems
EXAFS	extended X-ray absorption fine structure
FT	Fourier transforms
FTIRRAS	Fourier transform infrared reflectance absorption spectroscopy
HOPG	highly ordered pyrolytic graphite
HREM	high-resolution electron microscopy
IECEC	Intersociety Energy Conversion Engineering Conference
IIT	Illinois Institute of Technology
ISE	International Society of Electrochemistry
LANL	Los Alamos National Laboratory
LBL	Lawrence Berkeley Laboratory
LEED	low energy electron diffraction
LEIS	low energy ion scattering
MEA	membrane electrode assemblies
NSLS	National Synchrotron Light Source

NMR	nuclear magnetic resonance
OPG	ordinary pyrolytic graphite
PDS	photothermal deflection spectroscopy
PECVD	plasma-enhanced chemical vapor deposition
PEFC	polymer electrolyte fuel cells
PEM	proton-exchange membrane
PEO	poly(ethylene oxide)
PTFE	polytetrafluoroethylene
pzc	point of zero charge
RDE	rotating disk electrode
RFP	Request for Proposal
SCE	saturated calomel electrode
SEM	scanning electron microscopy
SERS	surface-enhanced Raman spectroscopy
SFUDS	Simplified Federal Urban Driving Schedule
SNL	Sandia National Laboratories
SRPE	solid redox polymerization electrode
SSRL	Stanford Synchrotron Radiation Laboratory
STM	scanning tunneling microscopy
TBAP	tetrabutyl ammonium phosphate
TDF	perdeuterated tetrahydrofuran
TEM	transmission electron microscopy
TGA	thermogravimetric analysis
THF	tetrahydrofuran
TMPP	tetramethoxyphenyl porphyrin
TPD	temperature programmed desorption
UHV	ultrahigh vacuum
UPD	underpotential deposition
USABC	United States Advanced Battery Consortium
XANES	X-ray near edge absorption spectroscopy
XAS	X-ray absorption spectroscopy
XPS	X-ray photoelectron spectroscopy

SUBCONTRACTOR FINANCIAL DATA - CY 1992

Subcontractor	Principal Investigator	Project	Contract Value (K$)	Term (months)	Expiration Date	Status in CY 1992*
EXPLORATORY RESEARCH						
Advanced Zn/NiOOH Cells						
Acme Electric Corp.	M. Anderman	Secondary Zn/NiOOH	193	12	9-93	C
APPLIED SCIENCE RESEARCH						
Lawrence Berkeley Laboratory	E. Cairns, L. DeJonghe, J. Evans, K. Kinoshita, F. McLarnon, J. Newman, P. Ross and C. Tobias	Electrochemical Energy Storage	1765	12	9-92	C
Electrode Characterization						
Brookhaven National Laboratory	J. McBreen	Battery Materials	95	12	9-92	C
Corrosion Processes in High-Specific Energy Cells						
Illinois Institute of Technology	R. Selman	Corrosion Resistant Coatings	132	12	8-92	T
Environmental Research Institute of Michigan	T.Hunt	Secondary Batteries	105	12	9-92	C
Johns Hopkins University	J. Kruger	Corrosion	30	12	8-92	T
Components for Ambient-Temperature Nonaqueous Cells						
Case Western Reserve University	D. Scherson	*In Situ* Studies	86	15	8-92	C
University of Pennsylvania	G. Farrington	Polymeric Electrolytes	50	12	7-92	T
AIR SYSTEMS RESEARCH						
Metal/Air Cell Research						
Eltech Research Corporation	E. Rudd	Oxygen Electrodes	125	12	8-92	C
Case Western Reserve University	E. Yeager	Air Electrodes	150	12	4-92	T
Fuel Cell R&D						
Los Alamos National Laboratory	S. Gottesfeld	Fuel Cell R&D	1200	12	9-92	C
Brookhaven National Laboratory	J. McBreen	Fuel Cell Research	94	12	9-92	C

* C = continuing, T = terminating

I. INTRODUCTION

This report summarizes the progress made by the Exploratory Technology Research (ETR) Program for Electrochemical Energy Storage during calendar year 1992. The primary objective of the ETR Program, which is sponsored by the U.S. Department of Energy (DOE) and managed by Lawrence Berkeley Laboratory (LBL), is to identify electrochemical technologies that can satisfy stringent performance, durability and economic requirements for electric vehicles (EVs). The ultimate goal is to transfer the most-promising electrochemical technologies to the private sector or to another DOE program (*e.g.*, SNL's Electric Vehicle Advanced Battery Systems Development Program, EVABS) for further development and scale-up.

Besides LBL, which has overall responsibility for the ETR Program, LANL and BNL have participated in the ETR Program by providing key research support in several of the program elements. The ETR Program consists of three major elements:

Exploratory Research

Applied Science Research

Air Systems Research

The objectives and the specific battery and electrochemical systems addressed by each program element are discussed in the following sections, which also include technical summaries that relate to the individual programs. Financial information that relates to the various programs and a description of the management activities for the ETR Program are described in the Executive Summary.

II. EXPLORATORY RESEARCH

The major thrust of this program element is to evaluate promising electrochemical couples for advanced batteries for electric vehicles (EVs). Exploratory research was carried out on Zn/NiOOH and Na/polymer cells, and novel components for various versions of these cells were also investigated, as described in the Applied Science section of this report.

A. ADVANCED ZINC/NICKEL OXIDE CELLS

New approaches to extend the cycle life of **Zn/NiOOH** cells are underway that involve modifying the electrolyte composition. There is a strong incentive to develop a long-lived Zn/NiOOH battery, because it would exhibit superior performance and lower life-cycle costs, compared to Ca/NiOOH and MH/NiOOH batteries.

Zn/NiOOH Cell Studies

E.J. Cairns and F.R. McLarnon (Lawrence Berkeley Laboratory)

The purpose of this project is to investigate the behavior of Zn electrodes in alkaline Zn/NiOOH cells to improve their lifetime and performance. Efforts are underway to investigate the mechanism(s) by which the redistribution of active material takes place, and to evaluate means of minimizing or eliminating the redistribution, thereby increasing the electrode life. Other related studies include the investigation of electrode morphology changes, nucleation, passivation, and current density distribution.

Our earlier work demonstrated that KOH-KF, KOH-K_2CO_3 and KOH-KF-K_2CO_3 electrolytes can greatly extend the cycle life of 1.35-Ah Zn/NiOOH cells. The KOH concentration in these new electrolytes is about half that used in previous versions of Zn/NiOOH cells, which results in a five-fold reduction in the solubility of Zn species. The rate of Zn-electrode shape change is much slower in these cells, and cell cycle life can be increased to 450-800 deep-discharge cycles (which may be compared to 100-200 cycles in KOH electrolyte). When the new electrolytes were used, the final cell capacity was limited by the NiOOH electrode, and the Zn electrode showed only a modest extent of shape change. We have recently focused our efforts on methods to improve the NiOOH electrode capacity retention in these electrolytes. Experiments were conducted that illustrate how the amount of active material loaded into the pores of the NiOOH electrode substrate affects the electrode cycle-life performance. The Zn/NiOOH cell capacity retention and NiOOH electrode coulombic efficiencies have been found to be superior in cells containing NiOOH electrodes loaded at 1.3 g/cm^3 void space, compared to cells containing NiOOH electrodes loaded at 1.6 g/cm^3 void space. It was also found that cells which were interrupted during their cycle-life test, and resealed at 0.5 bar (instead of full vacuum) showed a dramatic recovery of lost capacities. This result suggests the important role that wetting phenomena may play in the maintenance of acceptable cell performance.

A possible mechanism for the slow NiOOH electrode capacity degradation in the novel LBL Zn/NiOOH cells is the precipitation of inorganic Ni-Zn salts, which may passivate the electrode. Ex *situ* spectroscopic data are being gathered to identify species that may be present. Based on this information, a practical method for improving the NiOOH positive electrode may be formulated. X-ray diffraction has been used to examine NiOOH electrodes cycled in Zn/NiOOH cells. The data have not been conclusive, however, perhaps because of a lack of long-range order in the NiOOH electrode. Infrared spectroscopy was also used. The Ni sinter was magnetically separated from the active material [$Ni(OH)_2$ and NiOOH] and a CsI mull was prepared. The resulting spectra were of only fair quality, probably because of optical limitations of the available equipment.

A 20-Ah Zn/NiOOH cell was constructed using NiOOH electrodes with an active material loading of 1.6 g/cm^3 void space (not an optimal loading density, as described above). The dimensions of the Zn and NiOOH electrodes were 15 cm by 15 cm, which is the approximate size that would be used in EV batteries. The cell contained KOH-KF-K_2CO_3 electrolyte and was sealed under a vacuum. A small piece of Pt catalyst was used to oxidize the small amount of H_2 gas liberated by the Zn electrode during charge, and steady-state pressure was maintained at less than 1 bar. The internal temperature of the cell was monitored during charge and during a one-hour 15-Ah discharge, and did not exceed 30°C, which is considered to be satisfactory. The cell dropped below 60% of its initial capacity after 185 cycles at 80% depth of discharge. The cell capacity was limited by the NiOOH electrode, and an *in situ* X-ray image of the Zn electrode showed only a modest extent of shape change.

PUBLICATIONS AND AWARDS

1. R. Jain, T. Adler, F.R. McLarnon and E.J. Cairns, "Development of Long-Lived High-Performance Zinc-Calcium/Nickel Oxide Cells," *J. Appl. Electrochem.* **22**, 1039 (1992).
2. T.C. Adler, F.R. McLarnon and E.J. Cairns, "Alkaline-Fluoride-Carbonate Electrolyte for Zinc/Nickel Oxide Cells," *R&D-100 Award* (1992).

Applied Research on Secondary Zn/NiOOH Cell Technology

M. Anderman (Acme Electric Corporation)

The objectives of this project are to evaluate the LBL electrolyte composition for extending the cycle life of Zn/NiOOH cells, and to develop Zn/NiOOH cells for EV applications. This project was initiated as a result of an award from a Request-for-Proposals that was issued by LBL in 1992.

Various combinations of positive (*i.e.*, sintered and fiber Ni structures) and negative (*i.e.*, plastic-bonded and fiber structures) electrodes are being assembled with an approximate capacity of 16 Ah. These cells will be cycled with either the LBL electrolyte ($KOH + KF + K_2CO_3$) or a standard electrolyte (8 M KOH + 0.5 M LiOH).

Plate Fabrication. The procedure for the manufacture of plastic-bonded Zn electrodes was successfully implemented. A Pb coating was electroplated on the Cu mesh (after mechanically etching the surface, soaking in 50% POSICLEAN C acid Cu cleaner, cold rinse) in 50% lead fluoroborate bath. The Pb loadings are typically 50 mg/cm^2 of geometric area for complete coverage of the Cu mesh.

Experiments to fabricate Zn fiber electrodes are still underway. Some difficulty was encountered in uniformly plating a Pb coating on the inside of the pores in the Cu-plated fiber plate. Experiments that involve elevated bath temperature, air agitation, and addition of a Pb strike prior to plating were ineffective. Methods involving electrochemical and chemical precipitation are currently underway.

Cell Formation. Cells 1A (sintered Ni positive, plastic-bonded Zn negative) and 3A (fiber-bonded positive, plastic-bonded Zn negative) have completed their formation cycles. Figure 1 illustrates the voltage characteristics obtained during the last (3rd) formation cycle of Cell 3A.

The results of the 3 cycles for cells 1a and 3a are summarized in Table 1. For each cycle the capacity (Ah) is listed for the charge, Ni discharge and total discharge.

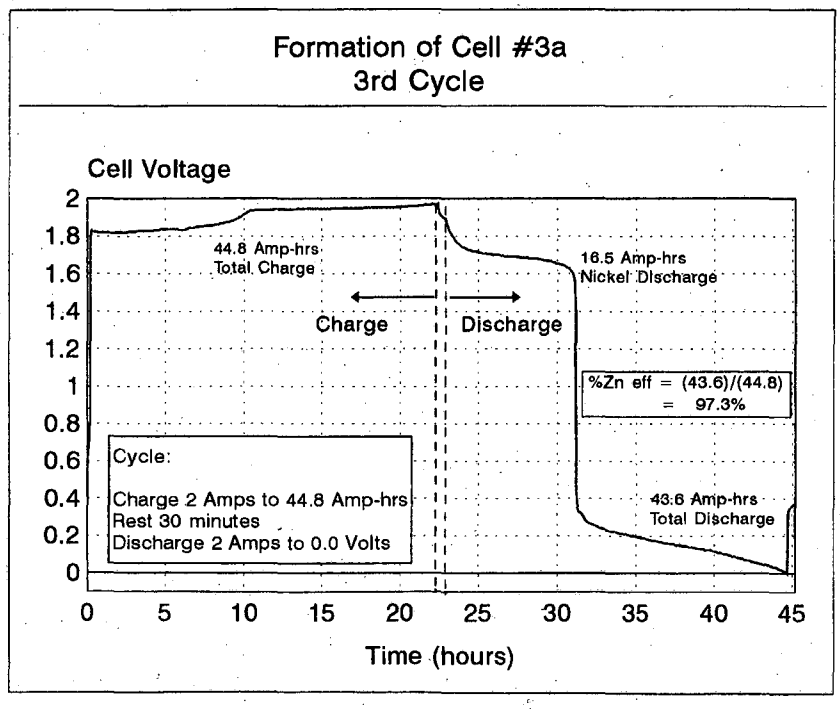

Figure 1. Voltage characteristics obtained during the last 3rd formation of Cell 3a.

Table 1. Formation Cycling of Zn/NiOOH Cells

Cell	1st Cycle				2nd Cycle				3rd Cycle			
#	Chg	Ni DChg	Total DChg	%	Chg	Ni DChg	Total DChg	%	Chg	Ni DChg	Total DChg	%
1A	40.0	22.0	36.7	92	40.0	22.7	38.9	97	40.0	15.6	27.3	68
3A	44.8	17.3	41.4	92	44.8	16.2	42.6	95	44.8	16.5	43.6	97

Cell 1A delivered only 68% of its total discharge capacity in the third cycle, and it was apparent from the cell-voltage characteristics that the cell developed a short. The voltage decreased to 1.12 V in two days. The results for Cell 3A are more encouraging; 97% total discharge capacity was obtained compared to 68% for Cell 1A. However, the Ni utilization is only 73% of its theoretical loading (22.7 Ah). Performance testing of this cell is continuing.

B. SOLID-STATE SODIUM/POLYMER CELLS

Efforts are underway to develop all-solid-state **Na/polymer** cells. The studies focus on demonstrating the viability of a sodium/sodium-alloy negative and a metal oxide positive in a rechargeable cell with a polymeric electrolyte.

Electrochemical Properties of Solid-State Sodium/Polymer Cells

L.C. DeJonghe (Lawrence Berkeley Laboratory)

The objective of this project is to investigate the viability of all-solid-state cells based on Na or Na-alloy negative electrode, polymeric electrolytes, and metal oxide positive electrode. Sodium or Na-alloy electrodes are attractive for use in solid polymer batteries because of their low cost and the wide availability of bulk Na, and the ease of fabrication of thin films which may lower the processing costs as well. Key research issues that are being addressed in this project are: (*i*) to identify the appropriate cathode materials, (*ii*) to investigate the intercalation of Na into a carbon host material, and (*iii*) to evaluate the transport properties of Na-conducting polymer electrolytes.

The P2 phase ($Na_{0.6}CoO_2$) was synthesized by the solid-state reaction of Co_3O_4 and Na_2O_2. Cells containing positive electrodes of the P2 phase, negative electrodes of Na or $Na_{3.75}Pb$ and poly(ethylene oxide) PEO were assembled in the half-discharged state ($Na_{0.6}CoO_2$), charged and cycled successfully. Sodium intercalates to a composition of $Na_{0.9}CoO_2$, and de-intercalated to a composition of $Na_{0.3}CoO_2$ (a total of 0.6 Na/Co), with no discernible phase change. The discharge curve is sloping, with an average voltage of about 3.0 V in Na cells (Fig. 2), and 2.9 V in $Na_{3.75}Pb$ cells (for 0.5 mA/cm^2). Cells can sustain current densities up to 2.5 mA/cm^2 for both charge and discharge, corresponding to the 1-2 C rate in Fig. 3, although there is some loss of capacity at the higher

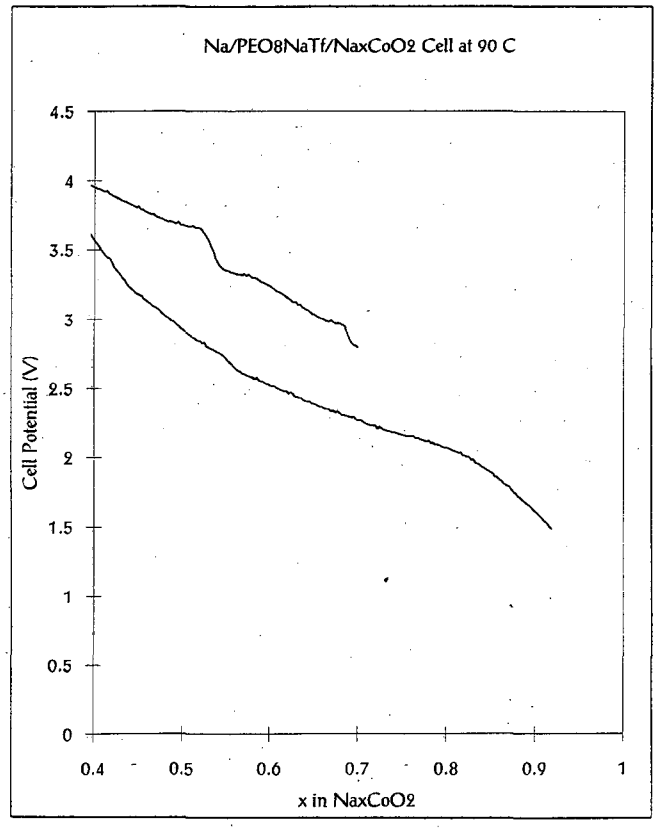

Figure 2. First cycle of a Na/P(EO)$_8$ NaTf/Na_xCoO_2 cell at 90°C. The current density was 0.5 mA/cm^2 for both charge and discharge.

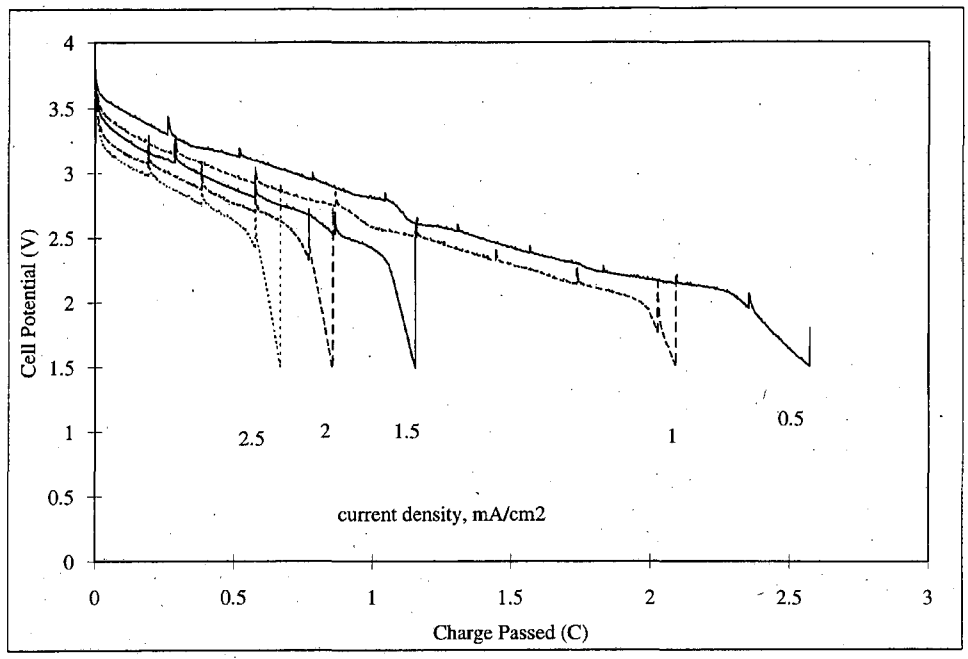

Figure 3. Discharge of $Na/P(EO)_8NaTf/Na_xCoO_2$ cells at various current densities from 0.5-2.5 mA/cm^2. The temperature is 90°C.

current densities. Over 100 cycles have been obtained at 0.5 mA/cm^2 to 50% capacity with the Na/sodium cobalt bronze system, and up to 200 cycles at somewhat shallower depths of discharge in Na and $Na_{3.75}Pb$ cells. Some loss of capacity is always seen upon cycling when a Na or Na-alloy negative electrode is used. A $Na_{0.6}CoO_2/PEO/Na_{0.6}CoO_2$ cell was cycled 250 times at 0.5 mA/cm^2 and exhibited similar capacity fading. This suggests that the cause of eventual cell failure may lie with the cathode, cathode/PEO interface, or less likely, with the PEO itself. X-ray diffraction on a spent positive electrode shows some peak broadening, but otherwise there is no change from the patterns taken on fresh samples. A possible explanation for these observations is the breakdown of the Na_xCoO_2 particles without structural changes in the material itself. This may lead to disconnection in the composite cathode resulting in eventual capacity loss. If this is true, the addition of electronic additives such as polyaniline fibers may improve cycling. Another factor contributing to cell failure may be the gradual decomposition of the polymer electrolyte because of the high cell voltages achieved at full charge (4.2 V *vs.* Na, 4.1 V *vs.* $Na_{3.75}Pb$). Cyclic voltammetry experiments suggest that $P(EO)_8NaTf$ (Tf = trifluoromethanesulfonate) is stable to about 4.3 V (*vs.* Na); however, these experiments are always performed on a short time scale (seconds to minutes) and may not accurately reflect the conditions of actual cell charge. If high voltages do contribute to premature cell failure, it may be possible to chemically modify the sodium cobalt bronze to lower the voltage upon full charge. Substitution of Ni for some of the cobalt atoms (*e.g.*, $Na_xNi_yCo_{1-y}O_2$) should not disrupt the cobalt bronze structure (provided y is kept small) or the electrochemical behavior other than slightly lowering the voltage. Although the cell resistance in sodium cobalt bronze/PEO/Na or Na-Pb alloy does not increase appreciably upon cycling, corrosion of Na or irreversible changes in the Na/PEO interface cannot be ruled out as a factor in premature cell failure. Experiments on Na/PEO/Na cells show no increase in resistance upon cycling, suggesting that any corrosion layer formed is stable and somewhat conductive. However, when Na is plated onto Ni or stainless steel foils through PEO electrolytes, decomposition occurs rapidly (on the time scale used in cyclic voltammetry), suggesting that corrosion is significant. The presence of even trace amounts of water in any of the cell components may prejudice the results; however, it must be noted that all components are carefully dried in a vacuum, and experiments are performed in a glove box

with less than 1-ppm O_2. The effect of corrosion on cell lifetime is not yet known, and further experimentation (AC impedance, four-probe measurements, etc.) will be directed towards understanding this phenomenon.

It may be possible to substitute a Na-ion intercalating material for the negative electrode (*e.g.*, a rocking chair cell). Studies of electrochemical Na-ion intercalation into various carbons (most notably, graphite and petroleum coke) are underway (Fig. 4). In contrast to previous findings, Na intercalation into carbon was successfully achieved at LBL, but is found to be highly dependent upon the particle size and type of carbon, as well as the electrolyte used. Sodium can intercalate reversibly in Conoco petroleum coke cells with PEO electrolytes to a composition of NaC_{24} and to a lesser extent in microcrystalline graphite. Although there appears to be a small initial loss of intercalated ions upon the first discharge and charge, no further losses are encountered upon cycling. Sodium may also intercalate reversibly into petroleum coke with liquid electrolytes such as dimethoxyethane, but decomposition occurs when non-ether containing solvents such as propylene carbonate are used.

Several Na-ion rocking-chair cells containing petroleum coke anodes, PEO electrolytes and $Na_{0.6}CoO_2$ cathodes were assembled and cycled successfully at low rate (0.1 mA/cm^2), as illustrated in Fig. 5. Rocking-chair cells require careful optimization, but even these first attempts were successful, and indicate a

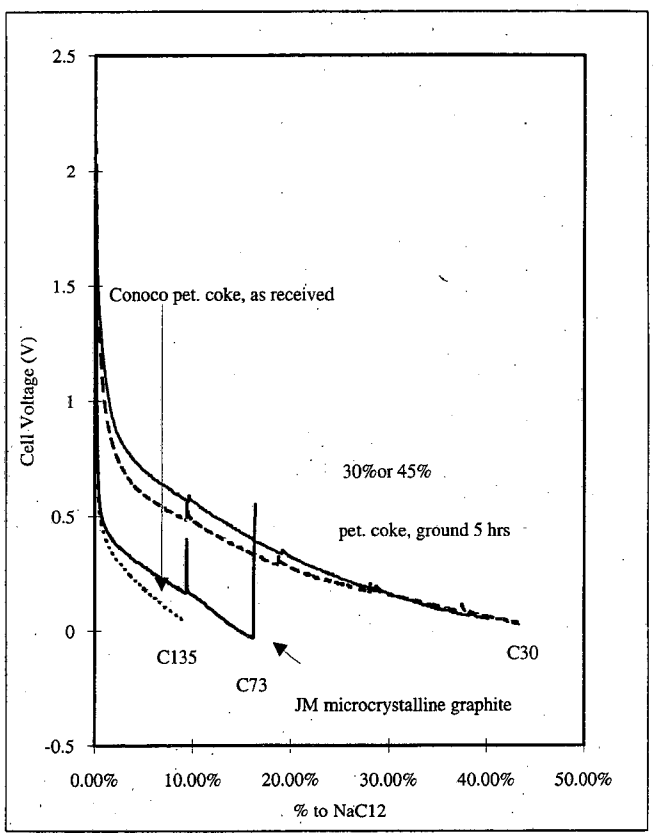

Figure 4. Discharge of Na into various types of carbon. Cells were of the configuration Na/P(EO)$_8$NaTf/C and were discharged at 0.025 mA/cm^2 and at 90°C.

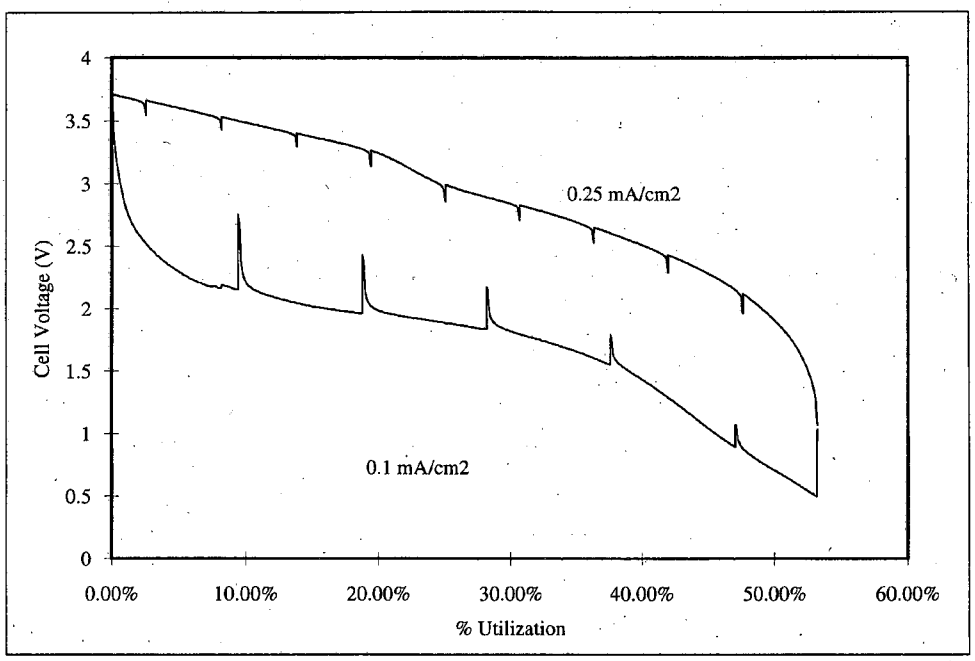

Figure 5. One cycle of a rocking chair cell, Na/P(EO)NaTf/C, at 90°C, charged at 0.025 mA/cm^2 and discharged at 0.1 mA/cm^2.

proof of the concept. Unfortunately, only half of the capacity in the $Na_{0.6}CoO_2$ electrode is available in the rocking-chair configuration. A better choice for a cathode material would be an intercalation compound that can be prepared in the fully discharged state. Furthermore, it should be a material with a rather high voltage and a flat discharge curve (*vs.* Na). Na_xMnO_2 compounds may very well fulfill all of these criteria and have the further advantages of being inexpensive and relatively non-toxic. Only a few incomplete studies of the behavior of MnO_2 in Na cells are reported in the literature, however. Therefore, some work in this laboratory will be directed towards the study of MnO_2 and related compounds in Na and rocking chair cells.

PUBLICATIONS

1. M.M. Doeff, S.J. Visco and L.C. DeJonghe, "Thin Film Rechargeable Room Temperature Batteries Using Solid Redox Polymerization Electrodes," *J. Electrochem. Soc.* **139**, 1808 (1992).
2. M.M. Doeff, M.M. Lerner, S.J. Visco and L.C. DeJonghe, "The Use of Polydisulfides and Copolymeric Disulfides in the Li/PEO/SRPE Battery System," *J. Electrochem. Soc.* **139**, 2077 (1992).
3. M.M. Doeff, C.M. Lampert, S.J. Visco and Y.P. Ma, "Solid Polyorganodisulfide Electrodes as Ion Storage Layers for Electrochromic Devices," *in Proc. of SPIE, Toulouse*, France, Spring 1992, Vol. 1728-06.

III. APPLIED SCIENCE RESEARCH

The objectives of this program element are to provide and establish scientific and engineering principles applicable to batteries and electrochemical systems; and to identify, characterize and improve materials and components for use in batteries and electrochemical systems. Projects in this element provide research that supports a wide range of battery systems: alkaline, flow, molten salt, nonaqueous and solid-electrolyte. Other projects are directed at research on improving the understanding of electrochemical engineering principles, corrosion of battery components, surface analysis of electrodes, and electrocatalysis.

A. ELECTRODE CHARACTERIZATION

Characterization of the electrode morphology and chemical composition are important for the successful development of rechargeable electrodes for advanced secondary batteries. Efforts are underway to utilize advanced microfabrication techniques and spectroscopy to characterize electrode properties.

Surface Morphology of Metals in Electrodeposition

K. Kinoshita and C.W. Tobias (Lawrence Berkeley Laboratory)

The objective of this project is to develop a pragmatic understanding of the component processes and their interactions in the macrocrystallization of metals necessary for the design and optimization of rechargeable galvanic cells. Other objectives are to elucidate the role of electrolyte convection as it affects overpotential behavior and ohmic resistance during gas evolution, and to clarify the effect of concurrent gas evolution on surface morphology in metal deposition.

During the initial stage of Zn deposition, the substrate is first covered with discrete nodules. In the presence of a flow field, these micron-scale nodules induce a hydrodynamic disturbance which enhances mass transport preferentially fore and aft of the protrusion. With continued deposition, the nodules align into striations that are parallel to the direction of flow. To quantify the magnitude of this hydrodynamic effect, the Navier-Stokes equations for viscous flow are solved numerically by the Boundary Integral Element Method (BIEM) for protrusion geometries with an axis of symmetry perpendicular to the electrode. The BIEM method reduces the problem to an integration over the profile of the protrusion and the wall in one dimension. So far only linear shear flows have been examined, but the solution can be applied to any uniaxial flow field. Future modeling efforts will include the effects of mass transport.

For experimental verification of numerical results, mass transport around hemispherical and cylindrical protrusions on the order of 100 to 500 microns in diameter will be studied using the limiting-current technique with a redox couple such as Fe^{2+}/Fe^{3+}. Electrically isolated Pt microelectrodes, which are smaller than the protrusion dimension (50-100 μm), are placed around the nodules so that detailed mass transport information can be obtained in the immediate vicinity of the obstacle.

It is a challenging task to integrate the large features required by the protrusion with the thin-film technology implemented in the Microfabrication Laboratory of the Berkeley campus. First, a small hole is drilled by a YAG laser in the substrate to be used for processing. Next, the microelectrodes are fabricated around the hole by a sequence of process steps that was developed earlier in this project. Finally, either a microsphere or a wire is placed in the hole to create a hemisphere or cylinder protruding from the surface. A new flow cell was designed and constructed for experiments with the segmented electrodes described above. The cell incorporates a flow duct of 3 mm x 3 mm cross section and 50 diameters of entrance length to ensure a fully developed flow.

Recent research efforts concerning electrolytic gas evolution phenomenon have addressed the impact of bubble coalescence and dissolved gas concentrations on these processes. Studies of coalescence dynamics in this laboratory by normal- and high-speed cinematography have demonstrated that because of the extremely short duration ($< 10^{-3}$-10^{-5} s) of each coalescence event, a more powerful technique is required. To quantify the coalescence rates between electrolytic bubble pairs, a laser projection apparatus was developed and is used in conjunction with an electrolytic cell containing precisely aligned, opposing microelectrodes in quiescent electrolyte (Fig. 6). A narrow sheet of laser light passes along the coalescence plane between the two bubbles. The interface formed

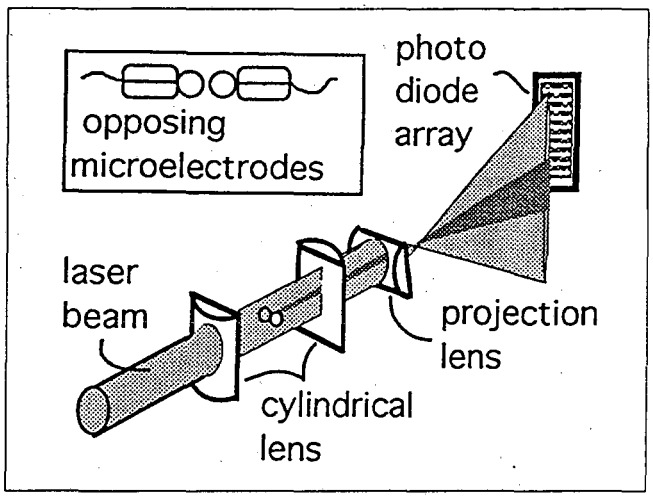

Figure 6. Schematic of electrolytic bubbles, laser optics and photodetector array for coalescence study. Isolated coalescence events between >500 μm electrolytically generated bubble pairs are resolved to $\pm 10^{-3}$ s.

between the bubbles upon coalescence creates a shadow which projects onto a high-speed, spatially resolving 16-element photodetector array. A dedicated data acquisition system samples the position of the shadow at regular intervals as short as 100 ns. The range of experiments to date was limited to 500- to 1000-μm diameter bubbles by the power of the laser and the sensitivity of the detector. Modifications have been incorporated to facilitate the measurements on more realistic bubble sizes of 50-500 μm, these include the use of a more powerful laser (1 W) and the improvement of the sensitivity of the detector circuit. A diagnostic study of the apparatus using a beam profilometer was conducted to quantify and minimize beam diffraction and other optical noise. Concurrent with the experimental study, a theoretical model is being developed for predicting coalescence behavior and for quantifying the impact of coalescence on local hydrodynamics and mass transfer. Further studies will include coalescence between bubbles of different size and composition.

Supersaturation of H_2 evolved on horizontal platinized Pt electrodes has been shown to increase with the square root of current density, indicating that surface renewal may be involved in the mechanism of mass transport. Current efforts extend the experimental observation to different bubble frequencies and sizes occurring on smooth Pt surfaces, thereby providing information necessary for establishing a definitive transport model.

Battery Materials: Structure and Characterization

J. McBreen (Brookhaven National Laboratory)

The objective of this project is to elucidate the molecular aspects of materials and electrode processes in rechargeable batteries and to use this information to develop electrode and electrolyte structures with good performance and long life. Work during the year included *in situ* EXAFS studies of Bi-doped manganese oxides and *ex situ* studies of lithium manganese oxides.

EXAFS studies of Bi-doped manganese dioxides: *Ex situ* EXAFS studies were initially done at the Bi L_3 edge on a series of Bi-doped manganese oxides and on manganese electrodes that were galvanostatically discharged in 9 M KOH to either one or two electrons per manganese atom. Spectra were also obtained for Bi foil, Bi_2O_3 and $NaBiO_3$. The XANES results indicate that the Bi in the charged electrode is in the Bi(III) state, but it is not Bi_2O_3. The EXAFS results indicate that the Bi is coordinated with both oxygen and manganese. There is some evidence for the formation of Bi_2O_3. Complete reduction by two electrons yields Bi metal in a finely divided disordered form.

In situ EXAFS studies were done at the Bi L_3 edge and the Mn K edge on Bi-doped manganese oxide electrodes in 9 M KOH electrolyte. The cells were cycled using a linear voltage sweep of 0.24 mV/s. The sweep was interrupted at several potentials and X-ray absorption spectra were recorded. Excellent data were obtained at the Bi L_3 edge. The data clearly showed reduction to Bi metal on deep discharge. On charge the Bi is oxidized prior to the onset of oxidation of the Mn active material. Initially the data at the Mn K edge were of poor quality because of excessive absorption of the X-ray signal by KOH and other cell components. A new cell was built to obtain data at the Mn K edge in the fluorescence mode. This solved the problem of background absorption by the electrolyte. A complete set of experiments were run at various stages of charge and discharge. Data were obtained at both the Mn K edge and the Bi L_3 edge. The quality of the data was excellent. The Mn results indicate that at the end of the one-electron discharge the manganese oxide is highly disordered. However, on completion of the two-electron discharge the product reverts to an ordered phase.

EXAFS studies of Li_xMnO_2 compounds: A series of Li_xMnO_2 compounds was prepared by sintering MnO_2 (CMD or EMD) with either LiOH or Li_2CO_3 at various temperatures. XAS spectra were obtained for

several of these compounds including $LiMn_2O_4$ and Li_2MnO_3. Spectra were also obtained for Mn, MnO, Mn_2O_3, Mn_3O_4, $KMnO_4$ and several types of MnO_2. The Mn XANES data indicate that the Mn in Li_2MnO_3 is in the Mn^{4+} state and that the Mn in $LiMn_2O_4$ has an average $Mn^{3.5+}$ state. The XANES also indicates that the Mn is in a more symmetrical environment in $LiMn_2O_4$ and Li_2MnO_3 than in either EMD or CMD. The EXAFS for EMD and CMD are consistent with a structure with a large amount of MnO_6 octahedra with shared corners. In the case of $LiMnO_4$ and Li_2MnO_3 there is no evidence for corner-shared octahedra.

PUBLICATIONS

1. J. McBreen, "EXAFS Studies of Battery Materials," *Proc. Symp. on X-ray Methods in Corrosion and Interfacial Electrochemistry*, A.J. Davenport and J.G. Gordon II, eds., The Electrochemical Society, Inc., Pennington (1992), pp. 214-226.
2. J. McBreen, "Characterization of Electrochemical Systems and Batteries: Materials and Systems," *Proc. of DOE Workshop on Advanced Battery Technology Research and Development*, A. Weber and K.M. Myles, eds., Division of Chemical Sciences, Office of Basic Energy Sciences, U.S. Department of Energy (1992), pp. 49-60.

B. COMPONENTS FOR HIGH-TEMPERATURE CELLS

Superior alternatives to the high-temperature sulfur-polysulfide electrode for Na/S cells are under investigation.

High-Temperature Cell Research

E.J. Cairns and F.R. McLarnon (Lawrence Berkeley Laboratory)

The objectives of this research are to investigate new electrodes, electrolytes and other cell components, and to determine the fundamental mechanisms of capacity loss of the electrodes, as well as means for eliminating the losses.

There are high-temperature cells available with acceptable lifetime and projected cost, but inadequate performance. In the specific case of the Na/S system, Na/S cells exhibit good performance (~180 Wh/kg), however Na/S battery performance is only marginal (80-100 Wh/kg). There is, therefore, a need to investigate more-energetic cell chemistries and seek improved cell designs. The addition of P to the S electrode is expected to result in improved specific energy, compared to Na/S cells, because of the low equivalent weight of P. Phosphorus/sulfur (P/S) ratios of 0.143, 0.332, and 1.17 were investigated, and the best cell performance was obtained with a P/S composition ratio of 0.143. This composition gave higher cell voltages, compared to Na/S cells, leading to a calculation of a theoretical specific energy 11% higher than that of the Na/S cell. Polarization measurements showed the P additive to reduce somewhat the cell performance under the restricted conditions of that experiment. Equilibrium cell EMF data from experiments using P/S ratios of 0.143 and 0.332, along with published data, were used to infer key aspects of the phase equilibria of the Na-P-S ternary system at 350 and 400°C. The studied region was the sulfur-rich corner of the ternary diagram extending to a Na mole-fraction of 0.4 and a phosphorus mole-fraction of 0.25. At least three three-phase regions appear to exist. Phase diagrams, which are consistent with the experimental and published data, were developed. These diagrams can be used in the design of experiments for further clarification of the phase equilibria of this little-studied system.

PUBLICATIONS

1. E.J. Cairns, F.R. McLarnon and P.L. Ridgway, "Sodium-Sulfur-Phosphorus Power Cell," U.S. Patent Assignment, Docket No. IB-910 (1992).
2. P.L. Ridgway, "Performance of Sodium/Phosphorus-Sulfur Cells and Phase Equilibria of Sodium-Phosphorus-Sulfur Mixtures," *M.S. Thesis*, LBL-33082 (1992).

C. CORROSION PROCESSES IN HIGH-SPECIFIC-ENERGY CELLS

These projects aim to develop low-cost containers and current-collector materials for use in nonaqueous, alkali-sulfur and other molten-salt cells.

Corrosion-Resistant Coatings for High-Temperature High-Sulfur-Activity Batteries

J.R. Selman (Illinois Institute of Technology)

The objective of this research is to develop corrosion-resistant coatings for cell components that are exposed to high-sulfur-activity environments in Na/S and Li/FeS_2 batteries. The efforts are directed at

producing dense and pore-free Mo_2C coatings on low-carbon steel by chemical vapor deposition (CVD), and to determine the correlation of coating quality with process parameters such as pressure (P), temperature (T), RF power, time (t), and gas flow rate.

Plasma-enhanced chemical vapor deposition (PECVD) is being used to prepare thin protective films at much lower temperatures than those required for thermally driven CVD. A lower processing temperature is required for PECVD because of the addition of plasma energy to the CVD environment in the form of a glow discharge, which creates highly reactive species. The effort has been to deposit Mo and Mo_2C films on a substrate of glass or steel.

Using an orthogonal factorial design, a series of experiments was carried out to investigate the effect of the evaporation rate of $Mo(CO)_6$ as a precursor. The chamber pressure was maintained at approximately 0.2 torr, although experimental parameters such as substrate temperature and RF were varied during deposition.

More information on the effects of chamber pressure, saturator temperature and substrate temperature were obtained by experimentation. The PECVD procedure was improved to minimize losses of $Mo(CO)_6$ in the reaction chamber. A series of experiments was carried out to investigate the effect of the leakage rate of the PECVD system, and the relationship between chamber pressure and operation time was deduced.

Analysis of the composition and microscopic morphology examination of the film were carried out. The thin film samples, which were deposited on glass and steel substrates, were submitted to McCRONE Associates, Inc. (Chicago) for analysis by X-ray photoelectron spectroscopy (XPS).

The samples were thought to be mainly Mo_2C, of a thickness somewhere on the order of a few hundred nm. For each sample, a full XPS spectrum was first recorded and the Mo was monitored. However, strong signals of oxygen and carbon as well as Mo were detected. The results showed an atomic concentration of 36.9% Mo, 18.8% carbon, and 44.9% oxygen on glass as substrate. The sample was then etched with an Ar beam at an etch rate between 1-2 nm per minute. After etching for 50 minutes, the atom concentrations were 55.5% Mo, 4.5% carbon and 40.1% oxygen. The etching for 50 minutes appeared to have removed a significant proportion of the film, revealing elements of the substrate in the spectrum. The thickness of the films is estimated to be in the range of 50-100 nm. Based on the XPS handbook, the results suggest that the thin film contains a molybdenum oxide.

To reduce the oxygen activity in the PECVD process, the use of H_2 and CH_4 as carrier gases in the reaction chamber are being considered. Hydrogen can reduce oxygen, accelerate the gas phase reaction and promote the decomposition rate of the precursor. Methane gas can also reduce oxygen and produce more carbon under reducing conditions.

Improved Container Electrode Coatings for Na/S Battery Systems

T. Hunt (Environmental Research Institute of Michigan)

The objective of this project is to develop improved corrosion-resistant coatings for high-temperature secondary batteries by sputter-deposition techniques. Research is underway to determine if properly prepared titanium nitride (TiN) coatings that are deposited on aluminum substrates can provide corrosion protection and durable electrical contact in the sodium sulfide environment of a Na/S battery. Previous experiments indicated that stoichiometric TiN films can provide a long-lived protective coating on Al substrates in a polysulfide bath.

A major effort was devoted to rebuilding the sputter-film deposition apparatus and investigating the conditions under which reasonably stoichiometric TiN films could be deposited. A series of TiN films were deposited by reactive D.C. magnetron sputtering (in which pure Ti is sputtered in an atmosphere containing a mixture of Ar and N_2) onto both Al coupons and glass cover slides. Over 60 samples with thin-film deposits were prepared. The nature of the stress in the deposited films on the glass cover slides was observed by their film stress-induced curvature. Neutral stress has generally been preferred to avoid film break up under the higher temperatures and corrosive environment present in Na/S cells. The deposited films span a range of compressive and tensile stress states and the stoichiometry was also varied, as judged primarily by the film color which has been a rather sensitive indicator in previous systems. The rate of TiN deposition was determined as a function of deposition conditions by measuring the thickness of the films deposited on glass microscope slides using a sensitive profilometer.

Corrosion tests are being initiated with samples of approximately 3-μm thickness. A simple static corrosion test apparatus was set up in the ERIM laboratory. The first TiNi-coated Al coupons were immersed in molten Na_2S_4 at 350°C for three weeks. Inspection of the coupons after the test showed the presence of a insulating aluminum sulfide layer when clean Al was

exposed to the melt and a conducting surface film on the side covered by the TiN layer. Microscopic and electrical evaluation of the first samples are underway, and corrosion testing of a second pair of samples is scheduled to begin shortly.

Corrosion, Passivity, and Breakdown of Alloys Used in High-Energy Density Batteries

J. Kruger (The Johns Hopkins University)

The objective of this project is to investigate the phenomena of passivation and its breakdown on metals and alloys in nonaqueous solvents for rechargeable Li batteries. The formation and the stability of passive films are important for the sustained integrity of construction materials used in high-energy batteries. This study is specifically concerned with the nature, formation mechanisms, and the mechanism of breakdown of passive films that exist on alloys in nonaqueous solvents.

The results obtained with 1018 carbon steel are similar to that observed with Fe in the DME systems with a few notable exceptions. The passivity of Fe or 1018 carbon steel is dependent on both the solvent and the electrolyte. In anhydrous DME with 0.5 M $LiAsF_6$, 1018 carbon steel displays an extensive and stable passive region up to 1100 mV (*vs.* SCE); Fe was passive up to 1300 mV. In this region several distinct passivation mechanisms are operative. Solvent chemisorption provides passivity up to 850 mV (SCE). Between 850 mV (SCE) and 1100 mV (SCE) another passivation mechanism appears to be operative in DME/$LiAsF_6$ solutions. The most plausible explanation of behavior in this potential range is that the DME solvent is chemically or electrochemically transformed, in the presence of AsF_6^- or a derivative, to a chemical intermediate that adsorbs on the carbon steel and provides a passive film. The sulfide inclusions on carbon steel may contribute to the breakdown of 1018 carbon steel in dry DME/0.5 M $LiAsF_6$ at lower potentials than Fe. Above 1100 MV on 1018 carbon steel and 1300 mV on Fe, a visible film was found on the bare surfaces; this film is caused by coverage by electropolymerization of the solvent. Small amounts of H_2O and $LiAsF_6$ salt act to enhance the polymerization process and expand the passive range. Chlorides in nonaqueous DME or in DME/H_2O mixtures did not interfere with the formation of the polymer on carbon steel. The polymerization does not proceed and the passive region is diminished when salts other than $LiAsF_6$ are used. In DME solutions containing tetrabutyl ammonium phosphate (TBAP) or $LiClO_4$ instead of $LiAsF_6$, the passivity was not stable above 700-850 mV (SCE).

Auger Electron Spectroscopy (AES) confirmed earlier results that iron and carbon steel formed a carbon-based polymer from DME during repassivation in a scratch at above the DME oxidation potential. For pure Fe in DME/0.5 M $LiAsF_6$ solutions, a reaction which has been confirmed as electropolymerization of the DME solvent takes place at 1300 mV (SCE). In dry DME/0.5 M $LiAsF_6$ solutions, polymerization takes place only when the Fe specimen is scratched down to the bare metal surface, which introduces Fe ions into solution. The electropolymerization of DME is dependent on the presence of $LiAsF_6$. In tests with Fe in DME saturated with $LiAsF_6$ the Fe passivates by polymer formation at the open circuit potential. Iron passivity is maintained up to at least 2700 mV (SCE) in saturated DME/$LiAsF_6$ solutions. It appears that the higher the salt concentration, the lower the applied potential required for polymerization to commence, and the better the polymer film in protecting the Fe surface. In dry DME/0.5 M $LiAsF_6$ solutions containing 50-100 ppm H_2O, polymerization takes place only when the Fe or carbon steel specimen is scratched down to the bare metal surface, thus introducing Fe ions into solution.

The passivation behavior of high-purity Fe and carbon steel was studied in binary DME/water mixtures. The results show that DME is the dominant species in the competition with H_2O for passivation in this binary system in solutions containing up to 70 mol% H_2O. In studies of pure Ni in dry DME/0.5 M $LiAsF_6$, passivity is maintained for several hundred millivolts above the passivity breakdown for Fe. Pure Ni acts almost as an inert electrode in DME/$LiAsF_6$, showing low passive currents until the salt decomposition reaction takes place. However, when $FeCl_3$ is added to the DME/$LiAsF_6$ solution, the Ni behaved like Fe in DME/$LiAsF_6$ solutions containing trace amounts of H_2O. Iron ions in solution are an integral part of the electropolymerization reaction.

In dry DME/$LiAsF_6$ solutions 304 stainless steel experiences breakdown at 1600-1650 mV (SCE) during potentiodynamic scans. Water additions above 1000 ppm tend to depress the breakdown potential toward 1200 mV (SCE) in DME/0.5 M $LiAsF_6$ solutions. Electropolymerization may be operative around 1700-2000 mV (SCE), but other competing processes may interfere in the formation of a passive layer. In DME with saturated $LiAsF_6$ a salt film appears to form in the bare areas at potentials around 1800-1900 mV. A polymer film was observed to form in DME/0.5 M $LiClO_4$ at 1900-2000 mV.

PUBLICATIONS

1. D.A. Shifler, P.J. Moran and J. Kruger, "The Passivity of 304 Stainless Steel in Propylene Carbonate Solutions," *J. Electrochem. Soc.* **139**, 54 (1992).
2. J.F. Scanlon, P.J. Moran and J. Kruger, "The Passivity of Iron in Anhydrous Dimethoxyethane and the Observance of Passivation by Electropolymerization," *Proc. of the Critical Factors in Localized Corrosion*, G.S. Frankel and R.C. Newman, The Electrochemical Society, Vol. 92-9, Pennington, NJ (1992).

D. COMPONENTS FOR AMBIENT-TEMPERATURE NONAQUEOUS CELLS

Metal/electrolyte combinations that improve the rechargeability of ambient-temperature, nonaqueous cells are under investigation.

Spectroscopic Studies of the Passive Film on Alkali and Alkaline Earth Metals in Nonaqueous Solvents: A Surface Science Approach

D.A. Scherson (Case Western Reserve University)

The main objective of this research is to elucidate the structure of passive films that form on alkali and alkaline earth metals in nonaqueous solvents. The main focus of the work conducted during 1992 was to investigate thoroughly the interactions between metallic Li, vapor deposited on clean polycrystalline silver (Ag(poly)), and condensed layers of perdeuterated tetrahydrofuran (TDF) at cryogenic temperatures. The preparation and characterization of these specimens were performed in ultrahigh vacuum (UHV) using Auger electron and X-ray photoelectron spectroscopies (AES and XPS, respectively), and temperature-programmed desorption (TPD) as probes of the elemental composition, electronic structure, energetics and mechanistic pathways of the reaction(s) involved.

All measurements were conducted in two independent UHV chambers. Lithium was vapor deposited onto clean Ag(poly) substrates from well-degassed SAES Getters sources. The purity of the bare Ag and Li overlayers was assayed by AES or XPS. The TDF (Icon Co.) and other gases were admitted into the vacuum chamber using a dosing system consisting of a capacitance manometer and a multicapillary array facing the sample. TDF (mass = 80) was used for most TPD measurements to distinguish hydrogen in THF from that which can be traced to other sources (hydrogen is the major background gas in UHV atmospheres).

The AES and XPS spectra of vapor-deposited Li layers on clean Ag(poly) were found to be in excellent agreement with those of clean Li reported by other workers (Figs. 7 and 8). Bare or Li-covered Ag(poly) substrates displayed no affinity for TDF at room temperature, as evidenced by the results obtained with AES, XPS, and TPD. Therefore all experiments were conducted with condensed layers of TDF at 120 K.

Both electrons and X-rays were found to damage the thick layers of TDF that condensed on either bare of Li-covered Ag(poly). In particular, areas of the specimen exposed to the electron beam during AES spectral acquisition were darkened considerably. Furthermore, the TPD spectra obtained using electron bombardment from the rear as the heating arrangement yielded features at temperatures higher than 300 K which were not observed when the same data were acquired with a resistive heating arrangement. Based on these considerations, all TPD experiments were conducted with the resistance heater, and the XPS spectra were recorded over short periods of time.

XPS Studies. The C(1s) and O(1s) XPS spectra for a freshly condensed layer of TDF (ca. 50 P thick) on Ag(poly) at 120 K displayed characteristic C(1s) features at 287.0 eV (C in C-C bonds) and 288.2 eV (C in C-O-C bonds) and one oxygen peak at 534.6 eV with integrated areas in good agreement with the TDF stoichiometry (see Panel 1, Fig. 9). Significantly

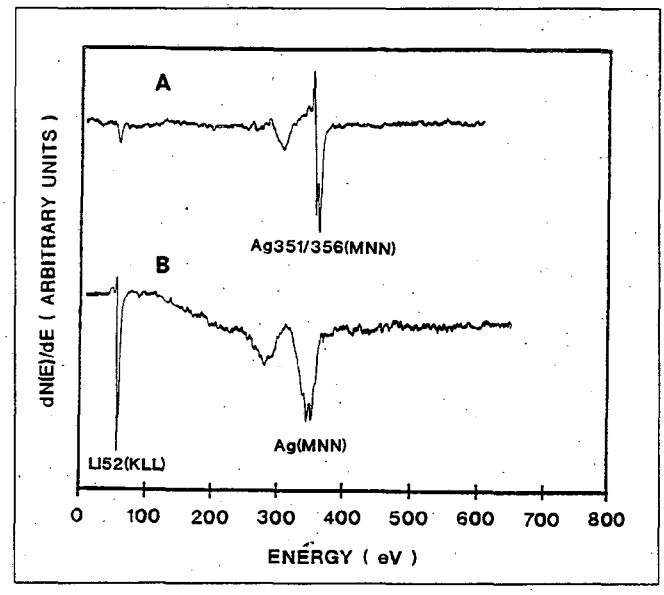

Figure 7. AES spectra of vapor deposited Li layers on clean Ag(poly) at 200 K at coverages of 50% (curve A) and 94% (curve B).

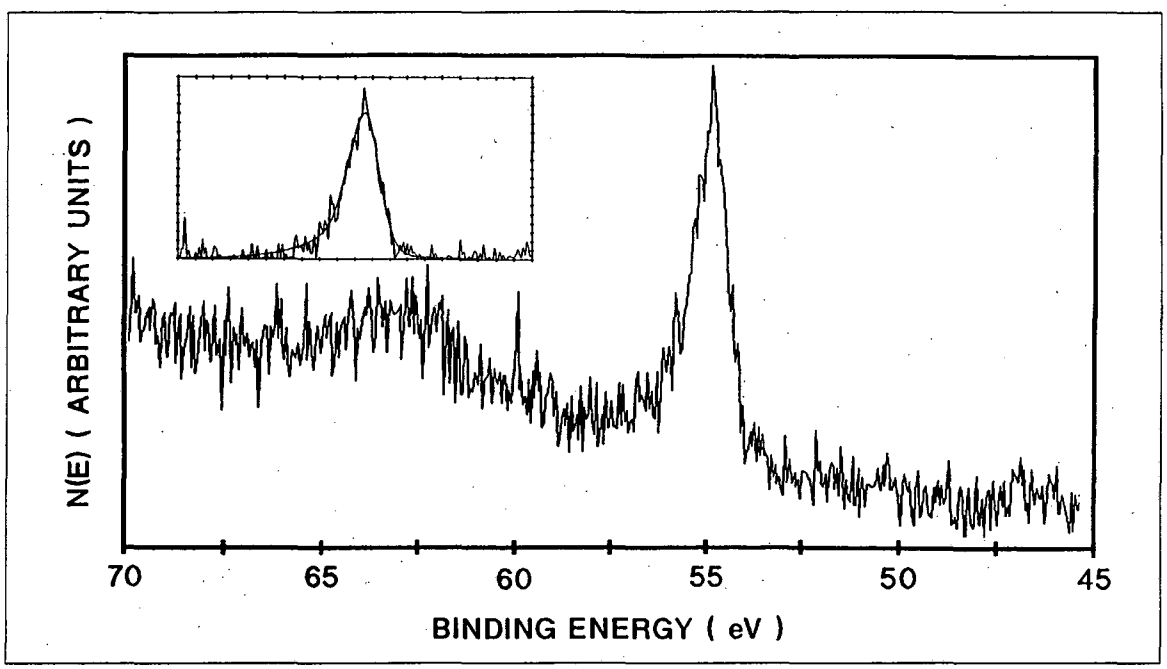

Figure 8. Li(1s) XPS spectra for a Li film deposited at 113 K. The inset shows the best fit to the Li feature.

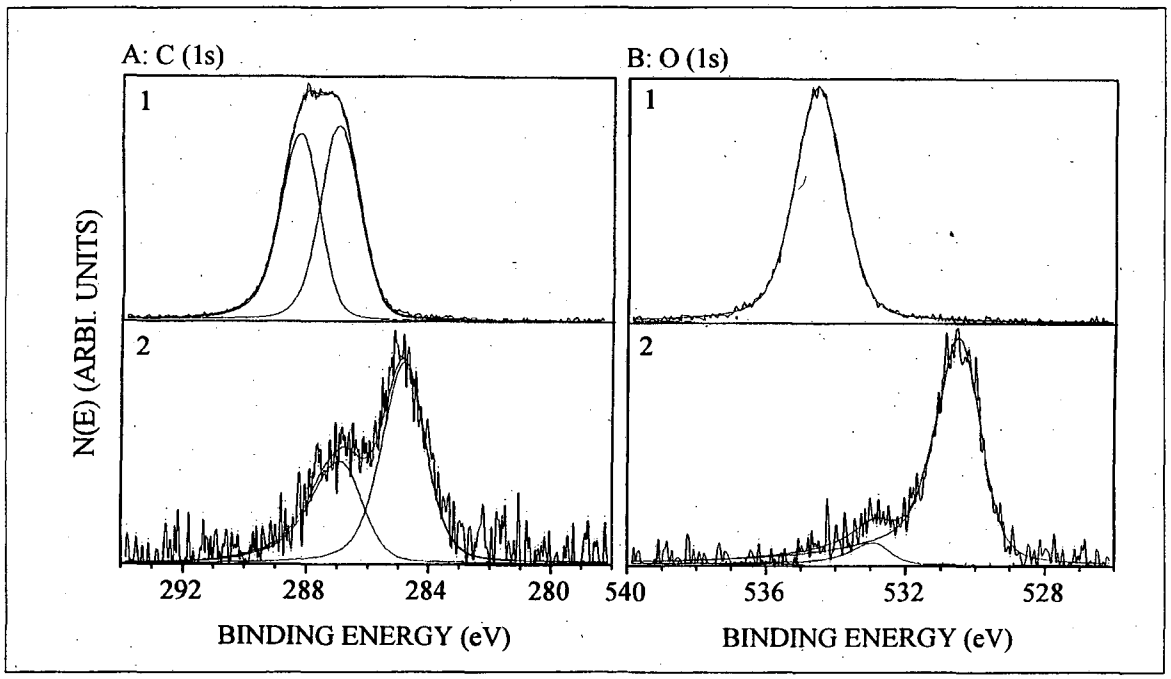

Figure 9. C(1s) [panel A], and 0(1s) [panel B] XPS spectra for a freshly condensed layer of TDF (ca. 50 P thick) at 113 K on 1. Ag(poly) and on 2. Li-covered Ag(poly) and subsequently warmed to room temperature.

different binding energies for C(1s) and O(1s) were found for TDF condensed on Li-covered Ag(poly) and subsequently warmed to room temperature (see Panel 2, Fig. 9). This indicates that the interactions between TDF and Li are strong, leading to substantial structural modifications.

TPD Studies. The TPD spectra for m/e = 48 with 15 L TDF condensed at 130 K on Li/Ag and on bare Ag are shown in Curves A and B, Fig. 10, respectively. Although the leading edge of the features obtained for both specimens are coincident within a wide range of temperatures, the width of the peak observed for the Li/Ag substrate, as well as the apparent integrated area, was about twice as large as that for bare Ag(poly). Except for the m/e = 28 peak, for which the amount observed for Li/Ag was about twice that measured for the bare substrate, these two types of specimens yielded essentially identical ratios for m/e = 48, 46, 30, 80, 78.

The most striking effect derived from the presence of the Li layer is the appearance of a sharp peak for m/e = 4 at 600 K which is associated with D_2 (see Curve A, Fig. 11) that is not observed on the bare Ag substrate (see Curve B, Fig. 11). Experiments in which Li/Ag surfaces at 300 K were exposed to H_2 (generated purposely by the Ti sublimation pump) yielded a TPD peak for m/e = 2 in the same temperature range. No such peak was observed for identical experiments involving bare Ag(poly) surfaces. Based on these observations and the fact that T_p is very similar to the temperature at which LiH undergoes decomposition it can be concluded that Li can dehydrogenate TDF to form LiD as one of the predominant products.

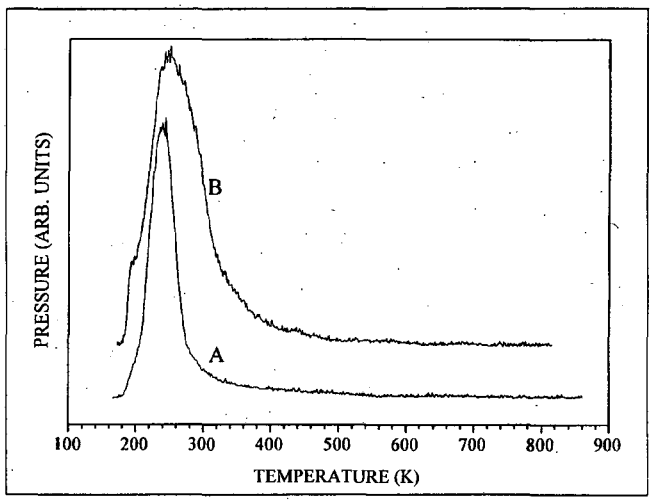

Figure 10. PD (m/e = 48) spectra for 15 L TDF condensed at 120 K on bare Ag(poly) [curve A] and Li-covered Ag(poly) [curve B]. Heating rate: 5 K/s.

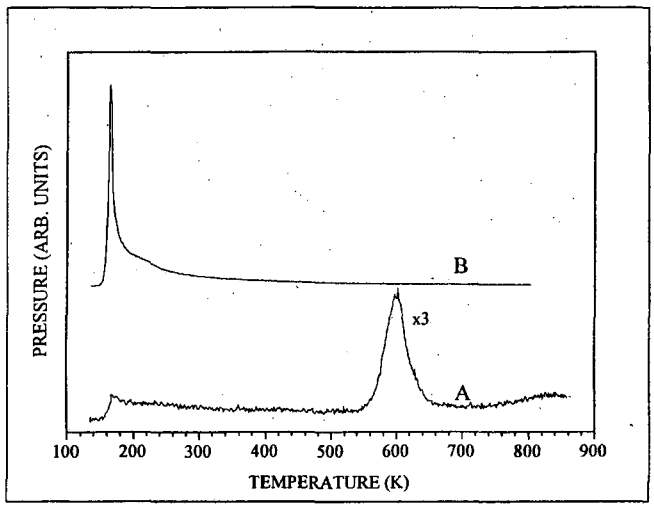

Figure 11. TPD (m/e = 4) spectra of 15 L TDF condensed at 120 K on Li-covered Ag(poly) [curve A]. The Li layer compared with 25 L TPD condensed at the same temperature on Ag(poly) [curve B].

In Situ Spectroscopic Applications to the Study of Rechargeable Lithium Batteries

D.A. Scherson (Case Western Reserve University)

The purpose of this project is to use *in situ* spectroscopic techniques to investigate the electrochemical phenomena that occur at Li/electrolyte interfaces during charge/discharge cycling. Two cell technologies are being considered, Li/polymer electrolyte and Li/FeS_2.

A better understanding of the changes in the structure and electronic properties of pyrite (FeS_2) and its corresponding lithiated derivatives (denoted generically as Li_xFeS_2, $0 \leq x \leq 2$), induced by the chemical and/or electrochemical insertion and removal of Li^+ ions from these materials is important to the further development of Li/FeS_2 batteries. With this in mind, *in situ* EXAFS spectroscopy of FeS_2 before and after electrochemical insertion of one and two lithium-ion equivalents, (Li^+)eq was investigated. These measurements were conducted in a specially designed spectroelectrochemical cell using components and electrolytes that are very similar to those used in primary Li/FeS_2 cells.

The cell used in these experiments consists of a thin Li anode, a separator, and a thin FeS_2 electrode arranged in a sandwich-type configuration. This geometry provides the optimal conditions for achieving a highly uniform current distribution so that the Li incorporation (or cell discharge) will occur

homogeneously over the entire FeS_2 electrode. In addition, the thickness of the complete assembly, which includes a thermally-sealed, aluminized, polymer-based casing to isolate the cell components from air, was sufficiently small so as not to appreciably attenuate the X-ray flux. This made it possible to acquire *in situ* EXAFS spectra in the transmission mode in a rather straightforward fashion.

In situ EXAFS spectra were collected for cells which were discharged to a depth-of-discharge equivalent to the insertion of one and two moles of Li per mole of FeS_2. During discharge, the cells were compressed with a C-clamp (which was removed prior to spectral acquisition) to decrease both the electronic (by promoting particle-particle contact) and ionic contributions to the IR drop. Throughout this procedure, the electrodes are always in contact with the electrolyte and current collectors; hence, the integrity of the cell, and therefore the *in situ* measurements are never compromised. The current densities during discharge were on the order of 0.5 to 2 mA/cm^2 to avoid high electrode polarization. All of the cells were assembled a few days before shipment to the synchrotron facilities and discharged immediately prior to the EXAFS experiments. The data were acquired at the National Synchrotron Light Source (NSLS) at BNL (Beamlines X18B; current: 110-220 mA, 2.5 GeV; monochromator crystal: Si<220>; step size: 0.77 eV (XANES), 0.05 A-1 (EXAFS)) and at the Stanford Synchrotron Radiation Laboratory (SSRL) (Beamline VI-2; current: 20-40 mA; monochromator crystal Si<111>; step size: 0.23 eV (XANES), 0.05 A-1 (EXAFS)).

Typical cell discharge curves are shown in Fig. 12 as a function of charge. During insertion of the two $(Li^+)eq$ (32.2 C/electron), the cell voltage dropped by only ~0.4 V, reaching ~1.0 V. The *in situ* k^3-weighted EXAFS spectra, obtained after zero, one and two electron discharge steps (curves a through c, respectively, in Fig. 13) revealed a gradual loss in the fine structure as the amount of Li in FeS_2 increased. These changes can be better visualized in the corresponding phase-shift-uncorrected Fourier transforms (FT) shown in Fig. 14. As indicated, the FeS_2 electrode before Li insertion (Curve a) displays features characteristic of pyrite, including pronounced peaks at 1.8 and 2.9 Å, attributable to the first two Fe-S shells (both with coordination number N = 6) and also at ~3.4, 5 and 6 Å assigned to the first three Fe-Fe shells in the lattice (N = 12, 6 and 24, respectively). After the insertion of one and two $(Li^+)eq$, the intensities of the shells with r' > 2.5 Å decreased monotonically compared to the major Fe-S peak.

A curve fitting analysis of the Fourier-filtered Fe-S backscattering ($k^3\chi(k)$) for the FeS_2 electrode before and after insertion of one and two $(Li^+)eq$ was performed with Fe-S phase and amplitude functions extracted from the first (Fe-S) backscattering in FeS_2. The resulting Fe-S interatomic distances, d(Fe-S), for FeS_2 after Li insertion, *i.e.*, 2.27 ± 0.02 and 2.29 ± 0.02 Å, for one and two $(Li^+)eq$, respectively, are significantly shorter that those reported for Li_2FeS_2, namely, 2.3737 and 2.4126 Å but very close to that for pyrite, for which d(Fe-S) = 2.250 + 0.005 Å.

The reduction in the S and Fe backscattering amplitudes upon incorporating Li^+ into FeS_2 strongly suggests that the most probable structure of the electrochemically formed material involves a highly disordered (possibly amorphous) form of $Fe_{1-x}S$ (with Li^+ counterbalancing the charge). Support for this view is provided by Mossbauer spectroscopy. Additional

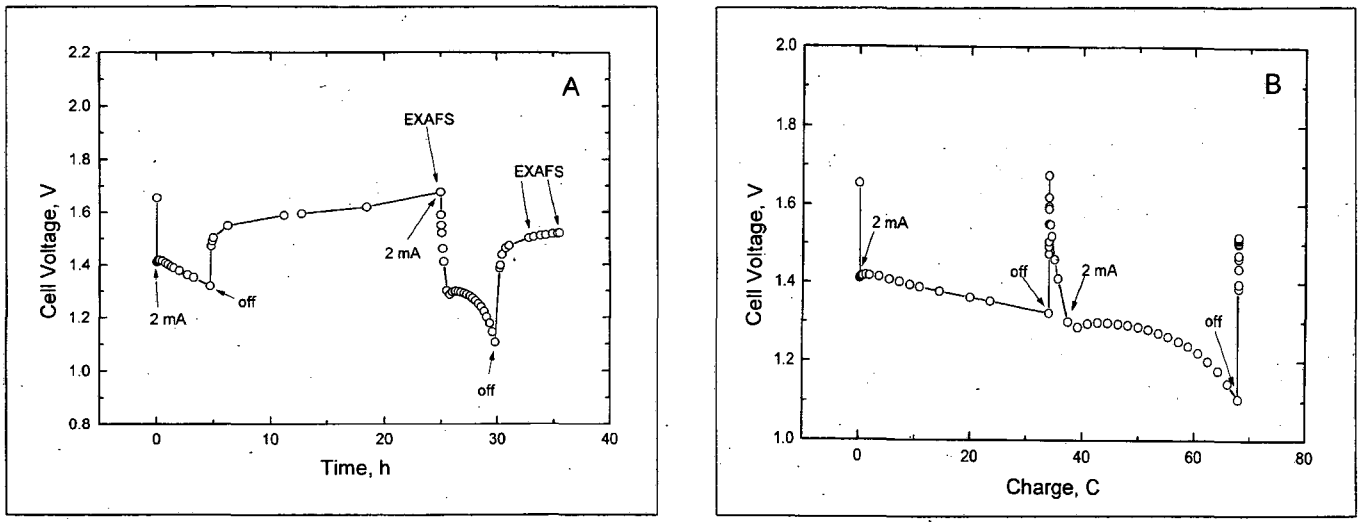

Figure 12. Cell discharge curves as a function of time (A) and charge (B). The precise times at which EXAFS spectra were collected are noted in B.

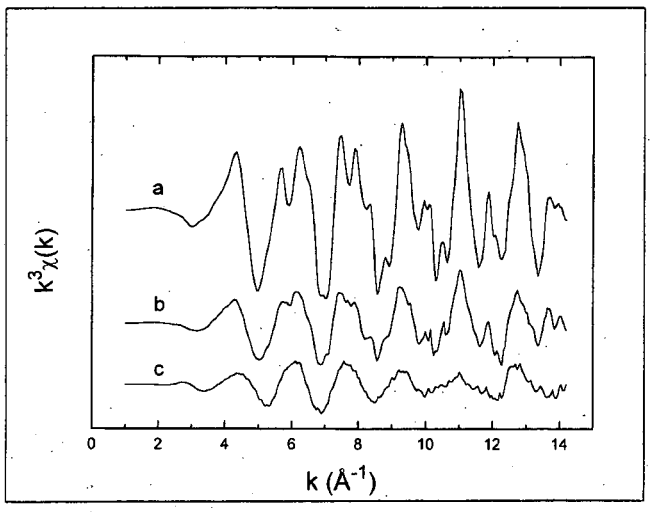

Figure 13. *In situ* k^3-weighted EXAFS spectra obtained during the various stages of discharge, zero (Curve a), 1 (Curve b) and 2 (Curve c) electron-discharge.

support for $Fe_{1-x}S$ as the most probable reaction product is provided by the XANES of the three specimens shown in Fig. 15. Despite the lower resolution of the highly structured near-edge region of crystalline pyrite, caused by the thick nature of the specimen, the insertion of Li^+ into the lattice leads, in addition to a much steeper edge jump, to a rounding of the XANES region. Such a lack of fine structure has been found in hexagonal $Fe_{1-x}S$. Also noteworthy, is the overall shift of the XANES toward lower energies as the amount of Li^+ in the lattice increases, an effect that is consistent with the gradual (electrochemical) reduction of the Fe centers.

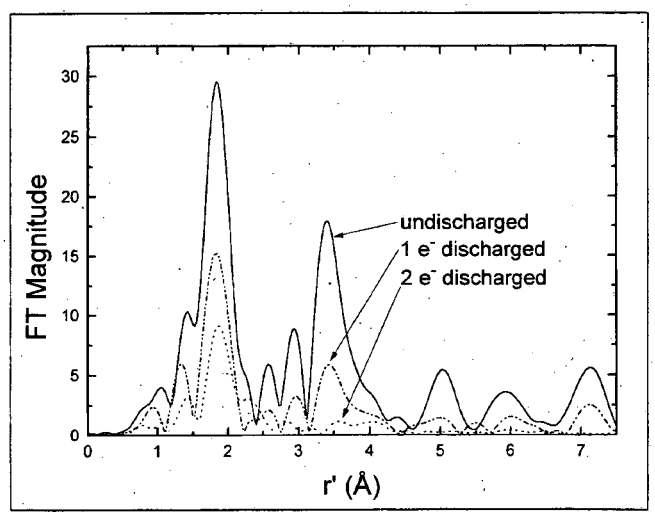

Figure 14. Fourier transforms for the stages of discharge specified in the caption for Fig. 13.

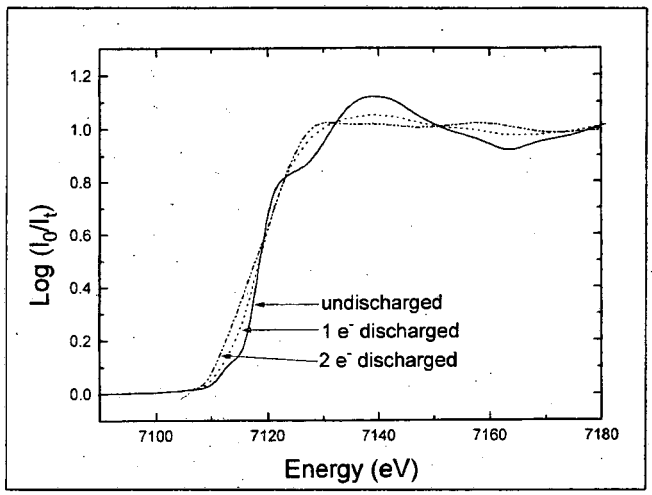

Figure 15. XANES for the stages of discharge specified in the caption for Fig. 13.

E. CROSS-CUTTING RESEARCH

Cross-cutting research is carried out to address fundamental problems in electrocatalysis, current-density distribution and gas evolution, solution of which will lead to improved electrode structures and performance in batteries and fuel cells.

Analysis and Simulation of Electrochemical Systems

J.S. Newman (Lawrence Berkeley Laboratory)

The objectives of this project include the investigation of efficient and economical methods for electrical energy conversion and storage, development of mathematical models to predict the behavior of electrochemical systems and to identify important process parameters, and experimental verification of the completeness and accuracy of the models. Results of this work are used to analyze experimental data, to identify important system parameters, and to aid in the design and scale-up of electrochemical systems.

Specific systems under study include the class of rechargeable Li thin-film batteries utilizing polymeric electrolytes, which are of interest for both EV and consumer applications. Current work in this area includes the development of general macroscopic models of single cells, modeling the thermal control of various battery configurations, and more detailed microscopic examinations of the behavior of electrodes in these cells during operation.

A general model for a cell containing a Li negative electrode, polymer electrolyte, and intercalation positive electrode was developed. The model is used to predict the behavior of the cell during charging and discharging. The generality of this model allows one to examine a wide range of particular systems that are currently being studied in the literature. The model was applied to the Li/polyethylene oxide/TiS_2 system. Detailed concentration profiles in the cell were generated and factors limiting the performance of the cell at high rates of discharge were determined.

A second model was developed to analyze the Li-ion "rocking-chair" system. The high reactivity of solid Li can be detrimental to battery performance because of the long-term degradation at the surface of the Li electrode. Similar to the first model, this model is general and can be used to simulate any combination of insertion electrodes and Li salt electrolyte. The particular system that was chosen for study included a carbon negative electrode, propylene carbonate solvent, and manganese dioxide positive electrode. Several interesting features of this cell system that do not appear with the solid Li system were examined and explained. A direct comparison of the two systems was also made, examining the effect of replacing solid Li with an insertion material on the energy and power of the system.

The models are being expanded to predict the thermal behavior of these systems during operation. This would allow one to predict heat-transfer requirements of the systems. Measurement of the transport properties of Li salts in Solid Polymer Electrolytes (SPE's) is underway to provide the data on transport properties that are crucial to the modeling effort. Another project that is just beginning involves a more detailed microscopic examination of the mechanism by which insertion electrodes used in these systems operate. Insertion electrodes, which are commonly metal oxides, operate by stabilizing Li atoms between layers of their structure. Because there is no bond formation, the electrodes are highly reversible and are often able to cycle many thousands of times. This fact, coupled with the wide variety of available materials, makes them very popular for Li battery applications.

The phenomenon of sustained oscillations in electrochemical systems is being examined. This phenomenon, involving an oscillation in the current being passed while a constant potential is held, is seen in a variety of systems, but usually occurs on electrodes that can form passive films which protect a metal surface from further corrosion. Experimental work being done with a model iron/sulfuric acid system has demonstrated the conditions under which oscillations occur, and a mathematical model is being developed to describe this behavior. A more fundamental understanding of this phenomenon will improve our understanding of passivation and oxide films in general.

Closely related to this effort is the development of a general model of oxide film growth that is nearing completion. This model is a highly detailed and rigorous treatment of the growth and transport of species through a metal/oxide/solution interface. In addition to corrosion applications, this model could be used to describe the growth of oxide layers on battery electrodes or in semiconductor processing.

PUBLICATIONS

1. T.F. Fuller and J. Newman, "Experimental Determination of the Transport Number of Water in Nafion 117 Membrane," *J. Electrochem. Soc.* **139**, 1332 (1992).
2. A.C. West and J. Newman, "Determination of Current Distributions Governed by Laplace's Equation," in *Modern Aspects of Electrochemistry*, B.E. Conway, J. O'M Bockris and R.E. White, eds., Pergamon Press, NY, 23,101-147 (1992).
3. T.F. Fuller and J. Newman, "Water and Thermal Management in Solid-Polymer-Electrolyte Fuel Cells," LBL-32769, August 1992.
4. S. Umino and J. Newman, "Diffusion of Sulfuric Acid in Concentrated Solutions," LBL-32770, August 1992.
5. M. Doyle, T.F. Fuller and J. Newman, "Modeling of Galvanostatic Charge and Discharge of the Lithium/Polymer/Insertion Cell," LBL-32769, October 1992.
6. C.A. Haynes, J. Newman, H.W. Blanch and J.M. Prausnitz, "Engineering Applications of McMillan-Mayer Dilute-Solution Theory," LBL-31973, September 1992.
7. A.J. Grabowski and J. Newman, "Current and Potential Distributions on a Cylinder Electrode," LBL-32539, December 1992.
8. M.-H. Wang, "The Electrical Conductivity of Sodium Polysulfide Melts," *M.S. Thesis*, University of California at Berkeley, 1992.
9. T.F. Fuller, "Solid-Polymer-Electrolyte Fuel Cells," *Ph.D. Thesis*, University of California at Berkeley, 1992.
10. B. Pillay, "Development and Application of the Quasi-potential Transformation," *M.S. Thesis*, University of California at Berkeley, 1992.

Electrode Surface Layers

F.R. McLarnon (Lawrence Berkeley Laboratory)

This research seeks to advance our understanding of the properties of surface layers on electrode materials that are important for the functioning of high-performance rechargeable batteries and fuel cells. The goal is to develop practical methods to form durable surface layers with predictable, superior properties, and to form these surface layers in a consistent manner in order to provide enhanced electrochemical cell operation. Continuing research is focused on the formation of oxides on metals that are used as the positive electrodes in rechargeable aqueous batteries, and previous studies on the corrosion of Pb-acid battery grid materials were completed.

Experimental observations of oxide formation are carried out by *in situ* spectroscopic ellipsometry, Raman spectroscopy, elastic light scattering, and scanning tunneling microscopy (STM). These observations are complemented by electrochemical measurements and different *ex situ* techniques of surface analysis. Information concerning the composition and micromorphology of surface layers is used in theoretical models of nucleation, growth and transformation of layers. Spectroscopic ellipsometry is used to determine spectral properties of surface materials and to derive wavelength-independent film structure parameters for which measurements at different wavelengths serve as independent monochromatic input. Film parameters are derived by the multidimensional optimization of optical models in which the difference between measurements and model predictions is minimized. Raman spectroscopy of surface layers for electrochemical characterization is conducted with equipment that is sensitive enough to observe unenhanced emission. This sensitivity is achieved by the use of a single monochromator, made possible by a multilayer filter for removing the incident and laser plasma wavelength and a channel-plate detector for observing the entire spectrum simultaneously. STM is used to determine surface topography with atomic-level spatial resolution.

Nickel Oxide Electrodes. In order to examine the interconversion between $Ni(OH)_2$ and NiOOH, and search for an effective way to improve the utilization of active material in Ni battery electrodes, the effects of introduced cations on the electrochemical behavior of the Ni electrode have been studied. Cobalt and Cu, two neighboring elements of Ni in the periodic table, were chosen as doping elements, and introduced into the surface layer of the electrode by using a metal-vapor vacuum arc ion implantation technique. The energy level of the implanted ions was controlled at 50 KeV, which corresponds to a ~10-nm penetration depth of implanted ions. This depth is comparable to the actual thickness of the $Ni(OH)_2$ layer formed on Ni substrates. Because of the good match between introduced and native atom lattice constants, the introduced cations are likely to be present as substituted, rather than inserted, atoms. The ion-implanted dose level ranges from 3.2×10^{15} to 7.0×10^{16} atoms/cm^2, and the expected ratio of introduced cations to native Ni atoms is ~20% when the dose level approaches ~10^{16} atoms/cm^2.

Both cyclic voltammetric and galvanostatic charge/discharge experiments on Co-implanted Ni electrodes have demonstrated that the potentials corresponding to the transformation between NiOOH and $Ni(OH)_2$ during both oxidation and reduction processes shift towards more negative values, compared with those of Ni electrodes without doping. In addition, Co-implanted electrodes appear to have a higher coulombic storage capability. The charge quantity released from a typical Co-implanted electrode is ~20% more than that of an undoped Ni electrode. However, Cu-substituted Ni electrodes show the opposite effect.

The LBL fast spectral-scanning self-nulling ellipsometer has been used to perform *in situ* characterization of the Ni electrodes with and without dopants during charge and discharge. Based on data analyses using an three-medium optical model and the effective medium theory, we have determined NiOOH volume fractions in the electrode surface layer by use of a numerical optimization process. The volume fraction of NiOOH for a Co-implanted electrode with a medium dose level can reach 90-95% after charging, which may be compared to ~80% for the undoped Ni electrode. This result indicates that the transformation between $Ni(OH)_2$ and NiOOH is facilitated by the introduction of Co cations.

It is expected that Cu-substituted electrodes will show the opposite effect, because of the different conduction mechanisms in the Ni electrode system. According to an analysis of valence states, Co and Cu dopants should function as donors and acceptors, respectively. Because NiOOH is commonly considered as a strong n-type semiconductor, and $Ni(OH)_2$ has poor conductivity, the introduction of donor impurities into the Ni electrode system can reduce the potential barriers at the boundaries between grains with different constituents, and thereby promote a more-complete transformation between $Ni(OH)_2$ and NiOOH. The experimental results also provide evidence to support the nodular growth model proposed earlier.

Lead-Acid Battery Grid Materials. Grid corrosion, particularly in the positive plate, is an important factor that limits the cycle life of lead-acid batteries. Surface modification by ion implantation has been investigated as a means to reduce the corrosion of grid materials. Pure (99.99%) Pb and a Pb-4%Sb alloy were chosen as representative grid materials. Titanium was primarily used for implantation, and the implantation of several other elements produced similar results.

Two methods were employed to determine the corrosion behavior of grid materials: (*i*) corrosion rates were derived from the current response of the specimens in 5 M H_2SO_4 electrolyte to small anodic polarization steps (3-10 mV), extrapolated from short-term measurements to zero time (to represent the behavior of the original surface); and (*ii*) the morphology of the corroded surface after extended (60-h) open-circuit immersion in 5 M H_2SO_4 electrolyte was determined by SEM examinations.

The lowest corrosion rates were obtained for the implantation of Ti into Pb and Pb-4%Sb with an energy of 60 KeV and a dose of 5.0 x 10^{16} atoms/cm^2. Under these conditions, the corrosion current is decreased by about 30-fold for Pb and by about 70-fold for the Pb-4%Sb alloy. Ion implantation with V, Cr, Ni or W also improves the corrosion behavior. Depth profiles of the implanted ions were obtained by AES. The profiles show a peak of Ti concentration at 40 nm below the surface (projected range).

PUBLICATIONS

1. R.W. Crocker and R.H. Muller, "Structural Transformation of Nickel Hydroxide Films During Anodic Oxidation," *Ph.D. Thesis*, LBL-32136, 1992.

Electrode Kinetics and Electrocatalysis of Methanol Electrooxidation

P.N. Ross (Lawrence Berkeley Laboratory)

The objective of this project is to develop an atomic-level understanding of the processes taking place in complex electrochemical reactions at electrode surfaces. Physically meaningful mechanistic models are essential for the interpretation of electrode behavior and are useful in directing the research on new classes of materials for electrochemical energy conversion and storage devices.

The relationship between the kinetics of electrode processes and the atomic structure of the electrode surface is being investigated. Processes under study include methanol oxidation electrocatalysis by ordered alloys, oxygen electrocatalysis by organometallic complexes and by oxides of novel composition and structure, and the corrosion of carbon electrode materials. Atomic-level structure determination is made using a variety of techniques, depending on the material under study: low energy electron diffraction (LEED) in the case of single crystals; low energy ion scattering (LEIS) for solid electrodes; high-resolution electron microscopy (HREM) in the case of carbon supported materials; and extended X-ray adsorption fine structure spectroscopy (EXAFS) in the case of organometallic catalysts.

The study of structure-related effects in electrocatalysis is a central theme in this research. Platinum surfaces which are modified by selected adatoms constitute the most active electrocatalysts for the direct electrooxidation of methanol. However, even the best of these catalysts suffers from very short lifetime and instabilities in performance. The basic mechanism of action of these adatoms remains speculative, and there is no rational basis for selecting one type of adatom over another. Recent work with single-crystal Pt surfaces has shown there are two unexpected complications of surface structure on the catalytic effect of adatoms: (*i*) the chemistry of the adatom is sensitive to the structure of the Pt surface; and (*ii*) the specific adsorption of ions in the supporting electrolyte on both the Pt surface and the adatom has a strong effect on catalytic activity. An understanding of these complex interactions with methanol electrooxidation kinetics is lacking.

The specific adsorption of anions in acid electrolytes containing H_2SO_4 and HCl was found to have a strongly inhibiting effect on the rate of methanol electrooxidation on both the (111) and (100) surfaces of Pt. The effect was much stronger in HCl, requiring approximately three orders of magnitude higher concentration of H_2SO_4 to achieve the same inhibiting effect (and surface coverage by adsorbed anion). The Cl^- adsorption isotherms were measured using the emersion technique and *ex situ* AES analysis. The mechanism of inhibition appeared to be similar for both anions. On the Pt(111) surface, anion adsorption was found to proceed in two stages, one coupled to hydrogen desorption producing a co-adsorbed state, and a second stage of adsorption at more anodic potentials into the anion adlattice from which hydrogen has been desorbed. The second-stage process on Pt(100) is different, occurring at more anodic potentials than on Pt(111) and concurrent with OH formation. Completion of the second stage of adsorption appears to produce the inhibition that causes a current peak to be observed in the voltammetry of

methanol in acids containing these anions. Underpotential deposition (UPD) of Cu in acids containing these electrolytes caused strong additional inhibition of methanol oxidation rate. The effect was attributed to induced anion adsorption on Pt atoms near to the UPD Cu atoms, which results in a lowering of the local pzc by the Cu adatoms.

PUBLICATIONS

1. P. Ross, "Trends in the Bonding of CO to the Surfaces of Pt_3M Alloys (M = Ti, Co and Sn)," *J. Vac. Sci. Technol.* **A 10**, 2546 (1992).
2. A. Haner, P. Ross, U. Bardi and A. Atrei, "Surface Composition Determination of Pt-Sn Alloys By Chemical Titration with CO," *J. Vac. Sci. Technol.* **A 10**, 2718 (1992).
3. N. Markovic and P. Ross, "The Effect of Specific Adsorption of Anions and the Underpotential Deposition of Cu on the Electro-oxidation of Methanol on Pt," *J. Electroanal. Chem.* **330**, 499 (1992).
4. H. Saffarian, P. Ross, F. Behr and G. Gard, "Electrochemical Properties of Perfluoroalkane Disulfonic Acids Relevant to Use in Fuel Cell Technology," *J. Electrochem. Soc.* **139**, 2391 (1992).
5. A. Atrei, U. Bardi, C. Rovida, M. Torrini and P. Ross, "Structure of the (001) Oriented and (111) Oriented Surfaces of the Ordered Alloy Pt_3Sn by LEED Intensity Analysis," *Phys. Rev. B* **46**, 1649 (1992).
6. U. Bardi and P. Ross, "Site Blocking Effect of Zirconium Oxide on the Pt(100) Surface: A LEED, AES and CO Thermal Desorption Study," *Langmuir* **9**, 132 (1993).

Effect of Electrocatalyst and Electrolyte Composition on Methanol/Air Fuel Cell Performance

E.J. Cairns and P.N. Ross (Lawrence Berkeley Laboratory)

Methanol has gained much attention as a potential fuel for many fuel cell applications, in particular transportation applications. The ease of storage and distribution, wide availability, and low cost of CH_3OH make it an attractive alternative to gaseous H_2, and the direct use of CH_3OH as a fuel eliminates the need for bulky/expensive reformers, which catalytically generate H_2 (for use as fuel) from a CH_3OH feed. The performance of electrodes employed in direct-methanol fuel cells is typically limited by slow electrochemical kinetics. The goals of this research are to characterize the kinetic and mechanistic behavior and to identify electrode structures, electrocatalysts, and electrolyte compositions that lead to improved performance in direct-methanol fuel cells (DMFC).

There is a strong incentive to investigate and characterize the performance of porous anodes and assess the roles of several physical and chemical parameters: electrode pore size and distribution; type, size, and distribution of catalyst (especially bimetallic catalysts); and electrolyte composition. Typically, the preferred catalyst is Pt supported on a carbon/Teflon structure. Prior investigations of combined catalysts, such as Pt/Ru, have shown promising synergistic increases in performance.

Model fuel cell experiments with Pt-Ru catalyst supported on graphitized carbon demonstrated a marked increase in performance over supported Pt for the oxidation of CH_3OH in concentrated Cs_2CO_3 electrolytes. The performance curves for Pt-Ru at 120°C match or exceed performance reported by others on Pt-black or supported Pt in concentrated Cs_2CO_3 at 120 to 150°C, and on supported Pt-Ru in concentrated H_3PO_4 at 200°C. In fact, these performance results are higher than any reported in the literature to date. Experiments were performed to evaluate the effect of various PTFE content levels in the porous-electrode reaction layer, and it was found that performance was maximized at 20-30 wt% PTFE. Similar experiments to evaluate the effect of temperature indicated that performance was maximized at 10 to 15°C below the boiling point of the electrolyte. The decrease in performance as the temperature approached the boiling point of the electrolyte was attributed to an increase in the water vapor pressure, which inhibited diffusion of the fuel and reaction products in the gas phase.

It has been reported that the method used to prepare carbon-supported electrodes, *i.e.*, heating in H_2, N_2 or air, has a major effect on electrode performance. Atomically resolved surface characterization is necessary to investigate these effects, and can be achieved by employing ultra-high-vacuum (UHV) techniques such as Auger electron spectroscopy (AES), X-ray photoelectron spectroscopy (XPS) and low-energy ion scattering (LEIS). For this purpose, we carried out research on smooth, polycrystalline Pt-Ru alloys of various compositions, enabling us to assess the chemical state of the alloys (oxide *vs.* metal) and their surface composition prior to electrochemical measurements, while maintaining atomically flat surfaces.

Our UHV analysis has established that annealing of Pt-Ru alloys in UHV or in H_2 produces surfaces which are strongly enriched in Pt. A similar phenomenon can be expected for carbon-supported catalysts, and the commonly reported optimum catalyst composition of 50% will very likely have a Pt-enriched surface. Electrochemical characterization of O_2-free Pt-Ru alloys in the presence of CH_3OH at 25°C in H_2SO_4 was carried out, and Pt showed superior electrocatalytic activity for fresh (unused) electrodes. Prolonged CH_3OH oxidation deteriorated its activity, but alloys with small amounts of Ru on the surface gave significantly better performance after a short time. An alloy with 10% Ru on the surface enhanced the oxidation of CH_3OH by a factor of 30, compared to Pt, and an alloy with a Ru surface concentration of 50% improved the activity of pure Pt by a factor of 10. This is in stark contrast to previous literature reports, where the optimum alloy composition was claimed to be 50% Ru. The high catalytic activity of small amounts of Ru indicate the high surface mobility of surface-bound CO, whose further oxidation most likely proceeds on Ru sites, whereas the adsorption of CH_3OH occurs exclusively on Pt atoms. Methanol adsorption, especially at low concentrations as envisaged in a DMFC, is a slow, often rate-limiting step and therefore an even larger surface concentration of Pt is required. This was also confirmed in our experiments in 0.005 M CH_3OH solutions. The implication for carbon-supported alloy electrodes is that new attention should be paid to investigating catalysts with low concentrations of Ru to possibly attain better performance in a DMFC.

Nuclear magnetic resonance (NMR) spectroscopy is a quantitative, non-destructive method of probing the chemical environment of a specific nucleus and has been used successfully in catalysis and surface science as a tool for identifying chemisorbed species. Because it is a bulk technique, NMR has been applied to systems very similar to practical catalysts. It is the goal of this research to extend further the application of NMR spectroscopy in order to obtain information on surface poisoning of graphite-supported platinum DMFC anodes in CH_3OH-containing H_2SO_4 electrolyte. Carbon monoxide has been postulated as the main poisoning adsorbate in the CH_3OH electrooxidation reaction, as suggested by *in situ* reflectance IR studies on smooth Pt electrodes. Our preliminary studies are therefore being concentrated on a model system of adsorbed CO. A probe for the observation of C^{13} magnetization has been built and tested and work on the model system is currently underway.

PUBLICATION

1. E.J. Cairns, K. Kinoshita, F.R. McLarnon and J.D. Rudnicki, "Photothermal Deflection Spectroscopic Studies of Electrochemical Oxidation," *Proc. of the Workshop on Direct Methanol-Air Fuel Cells, A.R.* Landgrebe, R.K. Sen and D.J. Wheeler, eds., The Electrochemical Society, Inc., Pennington NJ, Vol. 92-14, pp. 1-9, (1992).

IV. AIR SYSTEMS RESEARCH

The objectives of this program element are to identify, characterize, and improve materials for air electrodes; and to identify, evaluate, and initiate development of metal/air battery systems and fuel-cell technology for transportation applications.

A. METAL/AIR CELL RESEARCH

Metal/air cell research addresses O_2 electrocatalysis; bifunctional air electrodes, which are needed for electrically rechargeable Zn/air cells; and novel alkaline Zn electrode structures.

Electrocatalysts for Oxygen Electrodes

E. Yeager (Case Western Reserve University)

The overall objective of this research is to develop more effective electrocatalysts for O_2 reduction and generation which have high activity and long-term stability. Various electrocatalysts, including the transition-metal macrocycles and oxide catalysts, were evaluated to identify stable catalysts with much higher activity for both monofunctional and bifunctional air electrodes. This project was initiated on 1 April 1984 and completed on 30 April 1992. During that period numerous research topics related to the electrocatalysis of oxygen were considered, and some of the important specific accomplishments of this research are summarized here.

Transition Metal Macrocycle Catalysts

- Iron phthalocycanine (FePc) and its modified forms such as FeTsPc and FeTPyPz catalyze the 4-electron reduction of O_2 to OH- in alkaline solution when adsorbed on pyrolytic graphite at mono- or submonolayer coverages.
- Transition metals (*e.g.*, Co, Fe) adsorbed on heat-treated polyacrylonitrile (PAN)-based catalysts, particularly Co/PAN/XC-72, show promising performance for O_2 reduction in alkaline and acid electrolytes. These catalyst function through a peroxide mechanism similar to that involved with the heat-treated cobalt porphyrins and have comparable apparent activity.
- Heat-treated transition metal macrocycles such as CoTMPP dispersed on high-area carbon have high activity for O_2 reduction in alkaline and acid electrolytes, as well as good stability in concentrated alkaline solutions.
- Based on various electrochemical and non-electrochemical studies of the heat-treated macrocycles and related complexes, a model to explain the catalytic activity of the heat-treated transition metal macrocycles was proposed. The proposed model suggests a modified carbon surface on which transition metal ions are adsorbed, principally through interaction with residual nitrogen derived from the heat-treated macrocycles.
- Materials produced by the heat-treatment of pyrrole black mixed with transition metal salts are promising catalyst for O_2 electroreduction in both alkaline and acid electrolytes. Their activity is comparable to that of the corresponding heat-treated transition metal macrocycles on carbon.

Transition Metal Oxide Catalyst and Support

- Lead-ruthenate pyrochlores in the high-area form are found to be very active bifunctional catalysts for O_2 reduction and generation in concentrated alkaline solutions. They catalyze the 4-electron reduction of O_2 to OH^-.
- Pt catalysts supported on lead-ruthenate pyrochlore and with Nafion 117 (DuPont) membrane material pressed on the electrolyte side of the gas-fed electrode have shown promise for bifunctional O_2 electrodes in acid electrolyte (2.5 M H_2SO_4 at 60°C).
- Lithiated NiO powder has been used as a support for Pt-catalyzed gas-fed electrodes. The performance for O_2 reduction is inferior to using carbon supports in 5 M KOH at 25°C. This oxide has negligible activity for O_2 reduction at room temperature but has significant activity for O_2 reduction at temperatures higher than 150°C.

Transition Metal Macrocycle/Oxide Catalyst

- The perovskites have not generally been found to be active catalysts for O_2 reduction when used in O_2 cathodes either with or without high-area carbon. Some of the higher-area compounds have considerable activity for peroxide decomposition and O_2 generation. When used in conjunction

with heat-treated macrocycles, even those without a transition metal center, some of the perovskites show excellent performance for O_2 reduction.

- CoTsPc adsorbed on the perovskites $LaCoO_3$ and $La_{0.5}Sr_{0.5}MnO_3$ powders as catalyst supports has shown better activity for O_2 reduction as compared to that of the perovskite supports without the macrocycle in alkaline solution. The activity is much less than that of CoTsPc adsorbed on a high-area carbon under similar conditions.

Application of Experimental Techniques to Electrocatalysis Studies

- The combined use of FT infrared, laser Raman, TEM, Mossbauer, EXAFS, magnetic susceptibility, pyrolysis-gas chromatograph-mass spectroscopy, and linear sweep voltammetry of the adsorbed catalyst has provided new insight into the effects of heat treatment on catalyst stability.
- *Ex situ* and *in situ* Mossbauer spectroscopy has been successfully used to determine the state of the transition metal in macrocycles both in bulk and adsorbed on high-area carbon with or without subsequent heat treatment.
- FePc and its μ-oxo derivatives were characterized by FTIR, Mossbauer, STM, cyclic voltammetry, RRDE and gas-fed electrode measurements. It was found that the activity associated with th μ-oxo (1) species (crystallized from DMF solution) is comparable to that obtained with Powercat 2000 (a commercially available Pt-based high performance catalyst) in alkaline solution.
- Another class of compounds which has activity similar to the corresponding monomeric Pc, and is expected to have better stability in concentrated acid and alkaline electrolytes, is the polymeric Pc. Sheet-type CoPc and FePc polymers were synthesized, purified and separated from the low molecular weight fractions by dissolution in DMF. The high-molecular-weight fraction was characterized by FTIR, laser Raman, uv-visible and XPS measurements. The sheet-type configuration of the CoPc oligomer is evidenced by high-resolution TEM and atomic force microscopy (AFM)
- The orientation of the macrocycle complex on the surface has a strong effect on the activity as well as the pathway for O_2 reduction. *In situ* SERS, FTIRRAS and STM measurements of monomeric TsPc adsorbed on a substrate at mono- or submonolayer coverage provide evidence that the plane of the adsorbed TsPc complex is oriented at an angle to the surface. Polymeric sheet-type Pc, however, in the form of crystallites on a graphite surface show the sheet-shaped structure of the molecules that are stacked parallel to each other and parallel to the substrate by using AFM.

Carbon Supports and Porous Electrodes

- The stability of gas-fed O_2 electrodes in the reduction as well as generation modes has been enhanced using ion-conducting polymers in concentrated acid and alkaline electrolytes. This has been achieved by incorporating the ionomer in the active layer of the gas-fed electrodes and also by covering the solution side of the active layer with an ionomeric membrane.
- The fabrication of porous gas-fed electrodes was modified to optimize the use of such electrodes for stability and performance at high current densities in 85% H_3PO_4 at 100°C using carbon-supported Pt catalysts for O_2 reduction and generation.
- Generally, most of the high-area carbons used as support materials for catalysts are generally considered to be unstable for O_2 generation. Efforts have been made to find improved carbon supports. Several different carbon supports, including both oxidized and non-oxidized Shawinigan acetylene black, graphitized carbon and mildly fluorinated carbon black have been examined for use with lead ruthenate pyrochlore. All of these carbons gave similar performance. This is promising because it shows that highly oxidation-resistant carbons can be used without sacrificing cathode performance.

Mechanistic Studies of Oxygen Reactions

- Oxygen reduction to peroxide was examined in aqueous alkaline solution on highly oriented pyrolytic graphite (HOPG) with adsorbed 9, 10-phenanthrenequinone and on ordinary pyrolytic graphite (OPG) with chemically attached 2-amino anthraquinone. On the adsorbed quinone surface, the kinetics of the initial electron transfer (to the quinone) are fast while the reaction of the reduced quinone with the solution-phase O_2 is the rate-determining step. On the chemically attached quinone surface, the initial electron transfer is the rate-determining step because the quinone is farther from the surface and in an unfavorable configuration for electron tunneling.

- Oxygen reduction to superoxide was examined in acetonitrile on the basal planes of OPG and HOPG. The reaction has a lower apparent cathodic transfer coefficient on HOPG than OPG, probably due to part of the potential drop across the electrode/electrolyte interface occurring in a space-charge region in the HOPG. O_2 reduction to superoxide in DMSO was also studied on OPG, Au and Pt electrodes with and without CoTsPc in solution. The results indicate that CoTsPc does not catalyze the O_2 reduction to O_2^- in aprotic solvents, and the reaction appears to occur by an outer-sphere electron-transfer mechanism.
- The RRDE experiments showed that the reduction of O_2 proceeds by a 4-electron pathway on Ru. The kinetics and mechanism depend on the oxidation state of the Ru surface. The reaction mechanisms for the formation of the anodic film and O_2 reduction on the Ru metal were proposed.

Solution-Phase Voltammetry of Transition Metal Macrocycles

- The solution-phase voltammetric peaks for CoTsPc and FeTsPc in aqueous electrolytes have not been obtained so far. However, solution-phase voltammetric peaks were obtained in organic solvents. A possible explanation for this was based on the excess negative charge associated with the ligand in aqueous electrolyte as a result of the ionized SO_3^- groups attached to the four aromatic rings. The adsorption of such highly charged species on the electrode results in the repulsion of the corresponding solution-phase species. This explanation is supported by the effect of adsorbed TsPc on the redox behavior of negatively charged (ferri and ferrocyanide), uncharged (o-tolidine) and positively charged $Fe(ClO_4)_3$ in aqueous acid and alkaline solutions.
- To obtain further insight into the redox properties and O_2 reduction electrocatalysis on macrocycles, the effect of CN^-, capable of coordinating with the transition metal in the axial position, has been examined. The results indicate that a strong axial interaction of O_2 with the transition metal in the macrocycle is an important factor for O_2 electrocatalysis. The blocking effect of the voltammetric peaks confirms the assignment of the peaks in cyclic voltammetry curves and the importance of the particular redox couple to O_2 electrocatalysis.

Adsorption Studies of Transition Metal Macrocycles

- Adsorption of FeTsPc and CoTsPc on OPG has been investigated as a function of pH, and ionic strength of the adsorption solution and potential. Adsorption of CoTsPc occurs readily from its freshly prepared aqueous solution and is generally independent of pH. For FeTsPc, however, adsorption does strongly depend on pH. High surface coverage is achieved only from acid solutions rather than from pure water or alkaline solutions. This is explained in terms of the form(s) of the complexes existing in the solution phase in the presence of air.
- The PVP-modified OPG electrode with adsorbed CoTsPc exhibits higher activity for O_2 reduction than the OPG electrode with only adsorbed CoTsPc in 0.05 M H_2SO_4 solution. This is because of the formation of an adduct between PVP and CoTsPc which is more active and more stable than the CoTsPc. FTIR and uv-visible spectroscopic studies provide evidence for the formation of an adduct between CoTsPc and PVP.

Effect of Methanol on Oxygen Reduction

- To have more understanding about the redox properties and O_2 reduction electrocatalysis on transition metal macrocycles, the effect of alcohols such as methanol, isobutanol and n-amyl alcohol was examined. These alcohols may change the structure of the interface and orientation of the adsorbed macrocycles on the surface. The effect of methanol and its reaction intermediates on O_2 reduction are also of interest for the identification of methanol-tolerant electrocatalysts for O_2 reduction in methanol-air fuel cells. The half-wave potential ($E_{1/2}$) for O_2 reduction on CoTsPc, preadsorbed on an OPG disk electrode from its alkaline solution (~1 x 10^{-4} M) in the presence of these alcohols is more positive (~60 mV). This may be attributed to the increased adsorption of the macrocycle on the surface as a result of changes in the dielectric property of the solvent. The presence of ~1 M methanol in 2.5 M H_2SO_4 at 60°C showed no effect on the O_2 reduction performance using gas-fed electrodes based on pyrolyzed macrocycles (CoTMPP and CoTAA adsorbed on high area carbon). This is quite encouraging for the air electrode in methanol/air fuel cells containing acid electrolyte.

Novel Concepts for Oxygen Electrodes in Secondary Metal-Air Batteries

E. Rudd (Eltech Research Corporation)

The objective of this research is to develop improved bifunctional air electrodes for electrically rechargeable Zn/air cells. The successful development of bifunctional air electrodes depends on selecting electrochemically stable support materials and electrocatalysts for O_2 reduction and evolution, and the fabrication of suitable porous structures that are capable of extended operation. The present program is directed at investigating the viability of graphitized carbons and metal oxides in bifunctional air electrodes. Two carbon blacks, Shawinigan acetylene black and Cabot Monarch 120 furnace black, are being evaluated. After graphitization, these materials are used as the substrates to fabricate a series of active layers incorporating the following catalysts: *(i)* nickel cobaltite ($NiCo_2O_4$), *(ii)* cobalt oxide (Co_3O_4), and *(iii)* the pyrochlores $Pb_2Ru_2O_{7-y}$ and $Pb_2Ir_2O_{7-y}$.

A total of thirteen electrodes were fabricated; each electrode comprised of two layers, the active layer containing the materials described above and the gas supply layer, which were laminated together with a Ni mesh current collector. The gas supply layer was the same for all electrodes and contained graphitized Shawinigan acetylene black. The performance of the thirteen electrodes was determined in half-cell experiments using 5 M KOH as the electrolyte and a cyclic test regimen consisting of: (*i*) 2-h cathodic polarization at 20 mA/cm^2, (*ii*) 1-h open circuit, (*iii*) 2-h anodic polarization at 20 mA/cm^2, and (*iv*) 1-h open circuit.

The higher loadings used in some of the electrodes containing nickel cobaltite or cobalt oxide as catalysts did not provide a significant performance advantage. Furthermore, no immediate advantages were evident with Cabot Monarch 120 as the substrate rather than Shawinigan acetylene black. The cathodic polarization data, obtained periodically throughout the life of an electrode, indicated that the onset of flooding may be the primary cause of performance decline. It was also apparent that flooding did not affect the polarization behavior during the charging (anodic) cycle.

No significant difference was observed in the electrocatalytic activity of the lead ruthenate and lead iridate pyrochlores. Furthermore the activity was not as promising as reported in other studies. The activity of the lead iridate pyrochlore showed a gradual decline over 90 cycles which may be related to anodic oxidation of the electrocatalyst support. To minimize this problem an ionomer was incorporated in the electrode structure but this approach was not successful in eliminating the performance decline.

The anodic polarization behavior for all of the electrodes was surprisingly similar. This result suggests that the low surface areas of the pyrochlores (prepared by thermal decomposition) limited the activity of those catalysts. Efforts to lower the overpotential for oxygen evolution would be beneficial in terms of energy efficiency and could enhance the stability of the carbon black substrate.

Selected tests were also completed in small Zn/air cells (Zn flow-through electrode, 13-cm^2 electrode area) at MATSI Inc. (Atlanta, Georgia). The cells were operated at room temperature, using a different cycling regimen (discharge 4 h @ 10 mA/cm^2, charge 8 h @ 5 mA/cm^2) from that used in the half-cell studies, and the electrolyte was the low-alkali composition developed at LBL. An electrode with $NiCo_2O_4$ and Monarch 120 completed over 350 cycles in the single Zn/air cell. In contrast, both pyrochlores showed poor performance, and again, the presence of the ionomer in the active layer did not significantly improve the cycle life.

Transport in Zinc-Air Cells and Mathematical Modeling

J.W. Evans (Lawrence Berkeley Laboratory)

Efforts continue to evaluate the performance of a Zn/air cell that was developed at LBL. A major feature of this cell is its exploitation of natural convection to drive the electrolyte through the cell, saving on the weight, complexity, cost and energy expenditure of a pump. In the initial studies, a packed bed of Zn particles was used as the negative electrode which was recharged mechanically. The effort in 1992 demonstrated that solutal natural convection can also be exploited in other Zn/air cells such as the electrically recharged cell where Zn is present as a deposit on a Cu foametal. In the current design of Zn/air cell, the Zn is present as a coating on a porous Cu foametal substrate; this concept was originally demonstrated at LBL by Ross in a flow-through configuration where the alkaline zincate electrolyte was pumped (Ross cell).

Demonstrating solutal natural convection in the Ross cell entails three steps: (*i*) discharge of laboratory cells designed to achieve electrolyte flow by natural convection; the performance of these cells is being measured; (*ii*) measurement of electrolyte

velocities in the laboratory cells by laser-Doppler velocimetry; (*iii*) mathematical modeling of electrolyte flow, mass transport, reaction and current flow in Zn/air cells with the objective of providing an interpretation of the experimental results and as a tool for scale-up of the technology.

Laboratory cells (77 cm^2 air electrode area) were built for discharge of Zn on Cu foametal electrodes under conditions where electrolyte flow is driven by natural convection, rather than pumps. The discharge experiments were controlled by a microcomputer which permitted testing of the cells under SFUDS and other discharge regimens. Following discharge, the cells were electrically recharged at constant current. The results from a typical discharge using a BF-9 bipolar air electrode (Electromedia Corp.) are:

average current density = 20 mA/cm^2,
cut-off voltage = 0.8 V,
energy at cut-off = 3.96 Wh,
average voltage = 0.9 V, and
peak power at cut-off = 8.5 W.

These results are for discharge at 25°C. While this is only a moderate performance, various ways to improve it are already clear, for example, by eliminating most of the electrolyte volume in contact with the air electrode.

Measurements of the electrolyte velocity (in an electrolyte recirculation channel adjacent to the Zn electrode) by laser-Doppler velocimetry yields values of the order of 0.1 mm/s. There are upward velocities (with downflow through the Zn electrode) and have the magnitude, direction, and time dependence predicted by the mathematical model. The mathematical model predicts an electrolyte velocity that first accelerates from rest, on turning on the cell at constant current, followed by a gradual decline in velocity as the electrolyte approaches saturation and concentration differences driving the flow are reduced to zero.

PUBLICATIONS

1. J.W. Evans, G. Savaskan and T. Huh, "Further Studies of a Zinc-Air Cell Employed in Packed Bed Anodes. Part I: Discharge," *J. Appl. Electrochem.* **22**, 909 (1992).
2. J.W. Evans, G. Savaskan and T. Huh, "Further Studies of a Zinc-Air Cell Employed in Packed Bed Anodes. Part II: Regeneration of Zinc Particles and Electrolyte by Fluidized Bed Electrodeposition," *J. Appl. Electrochem.* **22**, 916 (1992).

Development of Electrically Rechargeable Zinc/Air Cells

E.J. Cairns and F.R. McLarnon (Lawrence Berkeley Laboratory)

The objective of this project is to develop the technology base to scale-up electrically rechargeable Zn/air cells for EV applications. Zn/air cells are tested under conditions that simulate typical EV use patterns.

The primary life-limiting component of electrically rechargeable Zn/air cells is the bifunctional air electrode. Perovskites, pyrochlores and spinel oxides have been suggested as bifunctional air electrocatalysts, *i.e.*, those that catalyze both the reduction of O_2 (during discharge) and the oxidation of H_2O to O_2 (during charge). The perovskite $La_{0.6}Ca_{0.4}CoO_3$ was shown to exhibit current densities as high as 3 A/cm^2 when combined with a high-surface-area carbon in a gas-diffusion electrode [Shimizu *et. al., J. Electrochem. Soc.*, **137**, 3430 (1990)]. We have focused on the preparation and study of bifunctional air electrodes based on this electrocatalyst.

Several techniques for the preparation of phase-pure $La_{0.6}Ca_{0.4}CoO_3$ powder with a high specific surface area and small, uniform particle size distribution were evaluated. The amorphous citrate precursor method yielded fairly pure powders with limited crystallinity and BET surface areas up to 18 m^2/g. A modification of this procedure, called the Pechini process, improved the particle size uniformity, but resulted in lower specific surface areas. An alternate procedure called the glycine nitrate combustion method involves rapid combustion of a stoichiometric mixture of metal nitrates with glycine fuel and leads to more highly uniform, but somewhat porous particles, however the specific surface area was not improved.

A procedure for the production of gas diffusion electrodes was developed. Gas supply and active layers were prepared by dispersion of PTFE-containing mixtures of graphitized carbon (plus catalyst for the active layer) with acetone, followed by kneading and rolling. The two layers were then rolled together with a Ni screen current collector, and dried and pressed at 340°C to sinter the PTFE. Variations in the procedure were evaluated by testing 1-cm^2 electrodes in a three-electrode cell. Larger (25 cm^2) electrodes were cycled in 0.9-Ah cells with reticulated flow-through, soluble Zn electrodes and an electrolyte composition of 45 wt% KOH and 40 g Zn^{2+}/l. The perovskite-catalyzed electrode achieved 45 cycles (to a cell cutoff voltage of

1 V), which may be compared with a macrocycle-catalyzed commercial electrode from Electromedia Co. that attained 72 cycles (C/6 charge rate, C/3 discharge rate). A key factor in the failure of these cells may be flooding of the air electrode, which is probably associated with the electrolyte carbonation caused by incomplete scrubbing of the inlet air. However, declining performance due to catalyst degradation cannot be ruled out. Other techniques for evaluating the performance and stability of transition-metal oxide electrocatalysts, such as cyclic voltammetry and measurements on oxide/carbon pastes in recessed disk electrodes, are under development.

The pulsed laser deposition technique (laser ablation) has been used to prepare a thin film of $La_{0.6}Ca_{0.4}CoO_3$ on a glassy carbon substrate, which was then made into a rotating disk electrode. This approach should enable measurements of O_2 reduction (OR) and O_2 evolution (OE) kinetic rate constants for comparison with other oxides on the basis of equal catalyst/electrolyte interfacial area. Preliminary studies on this film were carried out in 0.1-6.9 M KOH electrolyte, and the results indicated reasonable stability of the oxide films towards dissolution. Tafel slopes of 120 and 40 mV/decade were computed from mass-transfer-corrected current measurements in 6.9 M KOH electrolyte, for OR and OE, respectively. SEM analysis showed the film to be somewhat porous, and optimization of the deposition process to yield dense films is now underway with other substrate materials.

B. FUEL CELL RESEARCH

Fuel cell research includes projects in several areas of electrochemistry: fuel-cell testing, fuel processing, fuel-cell component characterization and theoretical studies.

Fuel Cells For Renewable Applications

S. Gottesfeld (Los Alamos National Laboratory)

The primary focus of this program is to develop efficient and cost-effective polymer electrolyte fuel cells (PEFCs) for transportation applications. The specific goals of the program are to: *(i)* reduce the cost of the Pt catalyst and ionomeric membrane, *(ii)* increase the efficiency and power density of PEFCs, *(iii)* optimize the system for operation on reformed organic fuels and air, *(iv)* achieve stable, efficient, long-term operation, and *(v)* solve key technical issues that impede the development of the direct methanol fuel cell (DMFC).

Thin-Film Electrode Fabrication using Thermoplastic Nafion. Significant advancements were made in the fabrication of thin-film catalyst layers for PEFCs. These thin-film layers which have ultra-low Pt loadings typically in the range of 0.10-0.15 mg Pt/cm^2 are applied to the ionomeric membrane either directly or by a decal method. In the previous fabrication techniques, heat treatment of the recast films (H^+ form of the ionomer) was necessary to impart robustness to the film. More recently, high-temperature casting of catalyst layers prepared with the Na^+ form of the ionomer was investigated, but also failed to achieve a crack-free, robust film with acceptable long-term stability.

Successful results were obtained by a process in which the thin-film catalyst layers are cast from an "ink" that consists of supported Pt catalyst and solubilized ionomer in the thermoplastic form of Nafion which is produced by incorporating tetrabutyl ammonium (TBA^+) by ion exchange. As before, casting of the thin films from solution provides a high degree of dispersion of the ionomer within the catalyst layer. When hot-pressed to the membrane (at 205°C and about 500 psi), the thermoplastic films are more robust and adhere more strongly to the membrane than with previous methods of fabrication. Prior to introduction into the cell, the catalyzed membrane is immersed in an acidic aqueous solution to reconvert the ionomer to the H^+ form.

Membrane/electrode assemblies (MEAs) prepared with the ionomer in the thermoplastic form exhibit an initial performance similar to that obtained with the H^+ or Na^+ forms of the ionomer (Fig. 16). However, the reproducibility achieved with the new process is significantly better, yielding uniform and defect-free catalyst layers. Furthermore, the long-term stability of these MEAs is significantly better than that exhibited by MEAs prepared with either the H^+ or Na^+ forms of the ionomer.

PEFC Life-Tests. The long-term viability of the thin-film PEFC catalyst layers was demonstrated in life tests. Several of these tests lasting between 2000 and 4000 h have been completed, and 90% of the initial performance was maintained for 4000 h of continuous operation in a PEFC employing 0.15 mg Pt/cm^2 on each electrode.

Life tests of PEFCs were performed at a constant cell voltage of 0.5 V, *i.e.*, close to the maximum power point of the cell. The cells were operated continuously at 80°C on pressurized, humidified air and H_2. The variation in performance with time for a PEFC based on thin-film catalysts using the TBA form of Nafion is shown in the upper part of Fig. 16. The performance of the cell has practically stabilized after the

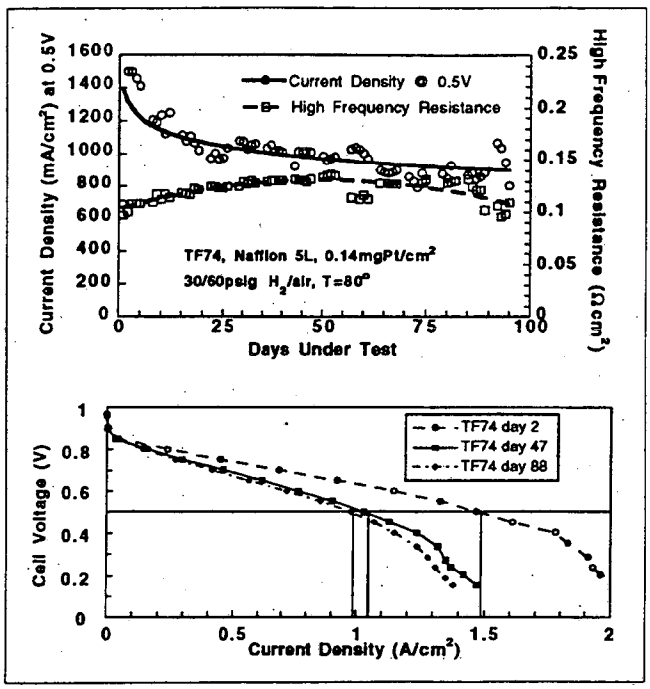

Figure 16. Top: Variations with time of cell current at 0.5V (upper curve) and of high-frequency resistance (lower curve) during a continuous 100 day test of a PEFC with thin-film catalyst layers of ultra low Pt loadings, operating on hydrogen and air. Bottom: Polarization curves for the same cell recorded at the beginning, middle and end of the life test.

first 1000 h of operation following an initial gradual decrease. The reason for the initial fall in performance is not believed to be attributable to the membrane electrolyte, because it maintained a relatively stable high-frequency resistance throughout the test.

As these life tests continued, we discovered that a large part of the cell performance losses recorded during the first 1000 h originated from an increase in the losses at the anode. This discovery was made during the study of the effect of low levels of CO, which were introduced into the fuel stream after 3000 h of test. The CO brought about a significantly lower performance. Subsequently, the addition of O_2 in the fuel not only completely removed the deleterious effect of CO, but the long-term performance loss was also recovered to a large extent (*i.e.*, bringing the performance after 3000 h back to the level of 90% of initial cell performance). This is illustrated in Fig. 17. Intermittent addition of air to the anode could subsequently sustain the performance at the level of 90% initial performance to the end of the 4000-h test. It is concluded that the origin of the initial (1000 h) performance loss (Fig. 16) is the slow poisoning of the anode catalyst. A low-level impurity in the (99.99%) H_2 gas cylinders is probably the origin of the slow poisoning. This highlights the sensitivity of the PEFC anode catalyst to very low levels of impurities in the fuel, however, they can be removed by *in situ* oxidation.

From the results in Fig. 17 we further conclude that the integrity of the thin-film catalyst based on the thermoplastic form of the ionomer is very satisfactory. Further support for this conclusion is provided in Fig. 18 which shows that, following the oxidative cleansing of the anode catalyst after 3000 h, there is practically no variation in the polarization curve when operating on O_2/H_2. Furthermore, only a small performance loss at high current density is observed after 3650 h with air/H_2. The small losses are attributed to the changes in the transport properties within the cathode catalyst layer and/or within the cathode backing.

PEFC Performance Losses Caused by CO_2. The apparent poisoning of the anode catalyst in PEFCs caused by CO_2 was studied. When steam-reformed CH_3OH is employed as the fuel, ppm levels of CO remaining in the post-treated reformate are known to cause anode catalyst poisoning. New reports from the GM/LANL program have suggested that deleterious effects in PEFC stacks could be caused by 25% CO_2 in the CH_3OH reformate. The PEFC stacks which showed this effect employed high (*e.g.*, 4 mg Pt/cm²) catalyst loadings. Two aspects of this important potential problem were consequently tested: (*i*) the degree of performance loss experienced by thin-film, ultra-low loading PEFC anodes in the presence

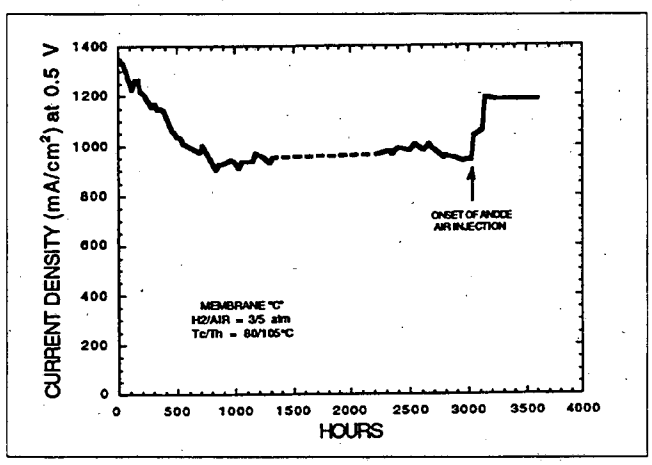

Figure 17. Long-term decay of PEFC performance, and its recovery by the bleeding of oxygen into the anode.

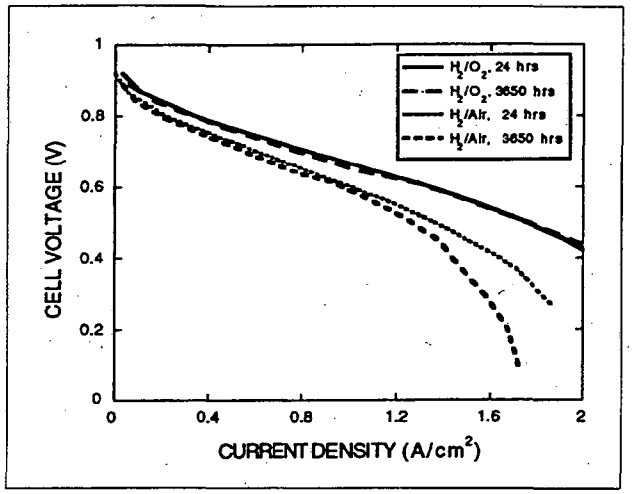

Figure 18. Polarization curves on H_2/O_2 (top two curves) and on H_2/air (bottom two curves) which demonstrate that, following anode cleansing by oxygen bleeding, no loss in overall cell catalytic activity is seen after 3600 h of operation with the thin-film catalysts. Only limited increase in mass transport barriers is detected in the air cathode after 3600 hours.

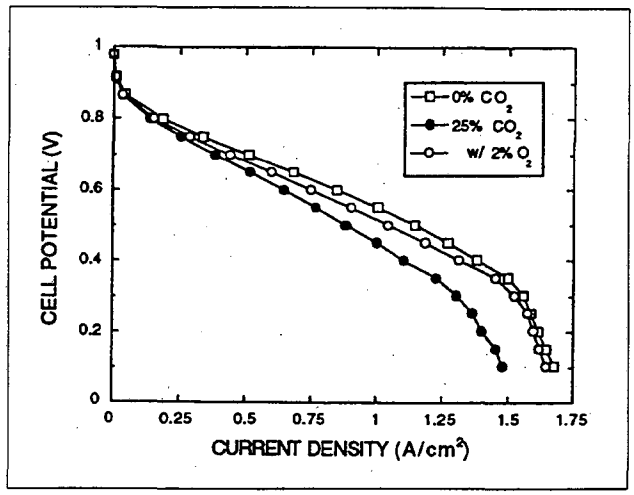

Figure 19. Deleterious effects caused by 25% CO_2 in the fuel feed stream (the CO_2 cylinder contained 2 ppm CO).

of 25% CO_2, and (*ii*) the removal of the surface poison by *in situ* reaction with oxygen.

In experiments conducted with PEFCs employing thin-film catalysts, the cell performance with an anode stream of 75% H_2 + 25% CO_2 was compared to the performance of the same cell with 100% H_2. The CO level in the CO_2 employed in these experiments was analyzed to be 2 ppm. The deleterious effect shown in Fig. 19 is only slightly higher than that expected with the 2 ppm CO in the fuel. Interestingly, the performance loss shown is significantly smaller than that reported for PEFCs of higher Pt loadings when operating on this type of fuel. Figure 19 also shows that adding 2% O_2 to the fuel effectively eliminates the losses in experiments with a fuel containing 25% CO_2.

To further clarify the effects of CO_2, a "prefilter" was added upstream of the PEFC. The prefilter consists of a (non-impregnated) gas-diffusion electrode with 0.4 mg Pt/cm^2, heated to 80°C. As the 75% H_2 + 25% CO_2 mixture passes through the pre-filter, the performance loss observed for the PEFC is significantly worse than that recorded without the prefilter. This result suggests that a higher Pt loading at the anode, particularly Pt in the form of metal exposed directly to the gas phase rather than coated by ionomer, enhances the formation of CO from CO_2 by the reverse shift process.

The following explanation is presented for the phenomena observed with fuel consisting of 75% H_2 + 25% CO_2. Two mechanisms for CO formation in the cell are:

$$CO_2 + H_2 \rightarrow CO + H_2O \quad (1)$$
(Reverse Shift)

$$CO_2 + 2H^+ + 2e^- \rightarrow CO + H_2O \quad (2)$$
(Electrochemical Reduction)

Internal generation of ppm levels of CO at the anode by one of these processes, or by both, could be sufficient to cause a significant deleterious effect. We suggest that the rate of reaction (1) is higher with higher Pt surface area in the anode, particularly that part of Pt catalyst exposed directly to the gas phase. This may be the reason for the greater deleterious effects of CO_2 in cells with higher Pt loadings. Oxidative cleansing of the internally generated, ppm-level CO can effectively take place at the Pt catalyst by employing a few percent O_2. The rate of this *in situ* oxidative cleansing also seems to increase with an increase in Pt surface area in the anode, particularly with catalyst area directly exposed to the gas phase.

Water Management and Ionomeric Membrane Characterization. Effort has concentrated on (*i*) testing of new ionomeric membranes, (*ii*) increasing the temperature to 80°C in membrane characterization experiments, and (*iii*) measuring the electroosmotic drag by protons in ionomeric membranes equilibrated with water vapor.

A membrane was received from DuPont designated Nafion 5L which is 3.5-4 mils thick and has an equivalent weight of 1000. This membrane has been recently renamed "Nafion 105" by DuPont. The specific protonic conductivity on the membrane is about 20% higher than that of Nafion 117 at the same temperature. Isopiestic equilibration of the 5L membrane at 30°C with H_2O vapor revealed a significantly higher H_2O uptake than that with Nafion 117. Most significantly, this membrane exhibits the smallest decrease in H_2O uptake we have observed when equilibrating with saturated H_2O vapor instead of liquid H_2O. At 30°C, Nafion 5L takes up 28 H_2O/SO_3H when contacted with saturated H_2O vapor, as compared with 14 for Nafion 117, Membrane C, and the developmental Dow membrane. This higher H_2O uptake from the vapor phase could provide a significant advantage in fuel cells humidified by H_2O vapor alone. Because this membrane is only half as thick as Nafion 117, this is a significant advantage in series resistance and water management in a fuel cell under load. The performance shown above in Fig. 16 is for a cell based on a Nafion 5L membrane.

The H_2O absorbed from the vapor phase by Nafion and other polymers at 80°C was measured. Our recent results (Fig. 20) indicate that Nafion 117 shows a substantial decrease in H_2O uptake at 80°C compared to 30°C. This difference is particularly pronounced at higher H_2O vapor activities. Previous reports have shown that the specific protonic conductivity of the ionomer in contact with saturated H_2O vapor passes through a maximum around 80°C. It is concluded that under equilibration conditions this maximum is a result of the opposing effects of enhanced protonic mobility and the decrease in H_2O content as a function of T.

The number of H_2O molecules dragged per proton transported across the membrane as a function of H_2O content in the membrane is critical for controlling the H_2O concentration profiles in PEFCs. Previously we measured this number with membranes in contact with liquid H_2O but not equilibrated with H_2O vapor. This year we have set up an apparatus similar to that recently developed by Fuller and Newman (F&N) for measurements of electroosmotic drag through membranes equilibrated with H_2O vapor. This measurement is based on the EMF developed between two edges of an ionomeric membrane, across which a well-defined H_2O activity gradient has been established by equilibration with two solutions of different H_2O activities. The lower limit of H_2O vapor activity was extended down to $a_W = 0.07$ in our measurements on Nafion 117 membranes by equilibrating the membrane with H_2O vapor above concentrated H_3PO_4. This extension was required to establish a result different than that reported by F&N. Our complete data, including the additional point for $a_W = 0.07$ ($H_2O/SO_3H = 1.4$), are shown in Fig. 21. Clearly a linear fit of the data on the semi-log plot is adequate down to the lowest water content. We thus conclude that in Nafion 117 the electroosmotic drag coefficient is constant, 1.0 H_2O/H^+, over a wide range of H_2O content, $2 < (H_2O/SO_3H) < 14$.

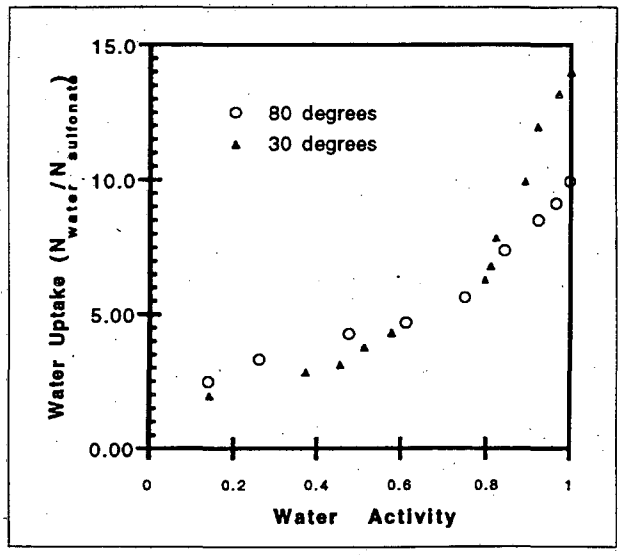

Figure 20. Water absorption isotherms for Nafion 117 at 30°C and at 80°C.

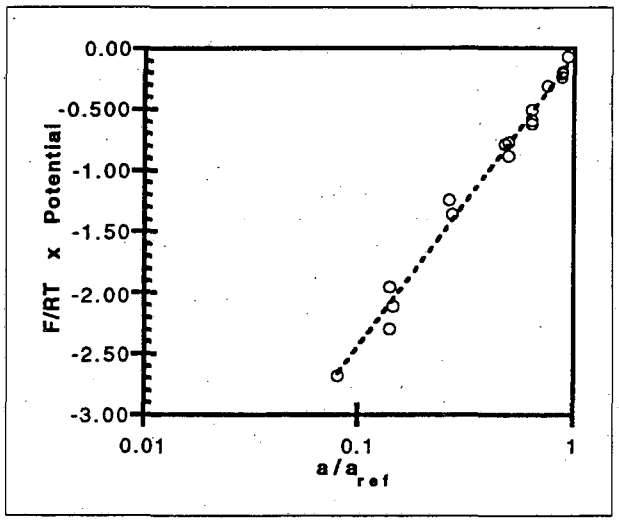

Figure 21. Plot of rational potential difference against log of water activity ratio for the EMF, water drag cell. The slope corresponds to a drag of 1.0 H_2O/H^+ through the water activity domain shown.

Direct Methanol Polymer Electrolyte Fuel Cells. A direct methanol/air fuel cell based on a polymer electrolyte (DMPEFC) was fabricated and tested. The fabrication of the DMPEFC employed the technique developed for the direct application of thin-film catalyst layers to the ionomeric membrane. A carbon-supported Pt-Ru (overall loading of 0.5 mg/cm^2) catalyst supplied by Johnson Matthey was used for the anode. A Pt/C catalyst (0.17 mg/cm^2) was used for the cathode. Thin-film catalysts were prepared from inks containing the catalyst powders, solubilized ionomer and glycerol.

The losses at the cathode of the DMPEFC caused by penetration of CH_3OH through the polymeric membrane was investigated. Methanol permeability has long been recognized as a very significant loss mechanism in DMPEFCs. The novel experiment performed to quantify this loss involved feeding the anode with mixtures of H_2 gas and CH_3OH vapor. When the anode feed contains such a mixture, the anodic current will be exclusively generated by the oxidation of H_2. No poisoning of the anode catalyst by CH_3OH oxidation should occur as long as the anode feed has a significant H_2 content. These measurements can also be used to probe directly the cathode loss in the DMPEFCs from CH_3OH permeating through the membrane. The results are shown in Fig. 22. It is apparent that the cathode losses increase from 20 mV with 1.2% CH_3OH to 150 mV with 45% CH_3OH in the anode feed. These results indicate that the flux of CH_3OH through the membrane is equivalent to 200 mA/cm^2, which corresponds to a concentration of 0.5 M CH_3OH in the membrane near the anode.

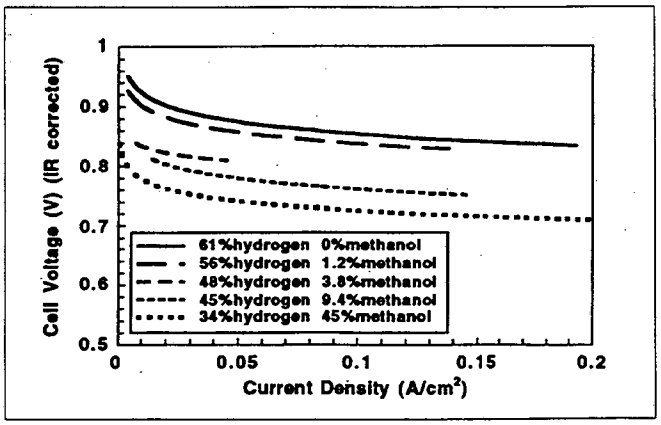

Figure 22. Effect of the methanol concentration in a mixed H_2/MeOH anode on PEFC performance.

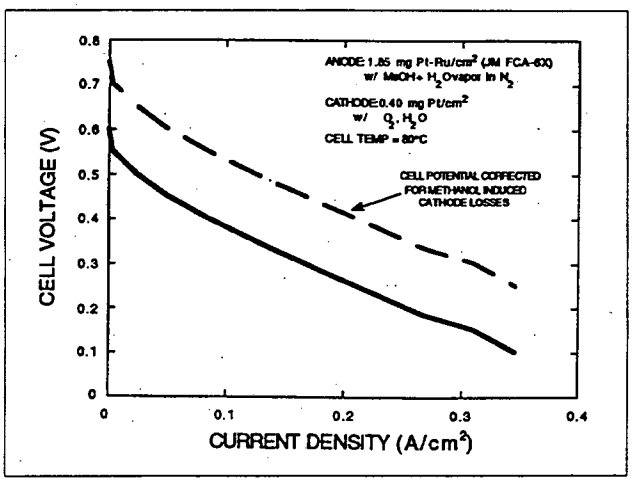

Figure 23. Polarization curves (raw result and corrected for cathode losses) for a direct methanol PEFC with an anode operating on a mixture of methanol and water vapors.

The best performance obtained in our tests of DMPEFCs with CH_3OH vapor is presented in Fig. 23. This figure shows that, with the mixture of CH_3OH vapor/H_2O vapor/N_2 (3-atm total pressure) at the anode, and with an O_2 cathode operating at 5 atm, current densities as high as 400 mA/cm^2 can be obtained at low voltage. The open circuit voltage is rather low, as expected because of the high CH_3OH permeation through the membrane and its reactivity at the cathode. The dashed curve in Fig. 23 shows the expected improvement in cell performance if CH_3OH in the membrane can be stopped from reaching the cathode.

A significant effort was devoted to identifying new membranes that have lower rates of CH_3OH permeation. This can in principle be accomplished in several ways by changing either the CH_3OH solubility or diffusivity or both. We have attempted to cross-link Nafion by γ-irradiation to reduce CH_3OH uptake, but the process appeared mainly to damage the membrane rather than introduce cross-linking. Membranes were prepared that contained sol-gel derived phases grown in the pores of Nafion. An optimum loadings has not been achieved, and some membranes are too stiff and poorly conductive while others lose the sol-gel phase when used in a liquid environment.

The CH_3OH diffusion coefficient in Nafion 117 which was emersed in neat CH_3OH and in a mixture of H_2O/CH_3OH was measured by NMR. A value of 1.2×10^{-5} cm^2/s was obtained at 30°C for the membrane exposed to pure CH_3OH. This value is about twice the diffusion coefficient of H_2O in Nafion under

the same conditions. Clearly, Nafion is very permeable to CH_3OH. The results obtained with the other sample exposed to a mixture of H_2O and CH_3OH was also very interesting. The diffusion coefficients of both H_2O and CH_3OH at 30°C are enhanced relative to those in pure CH_3OH. The self-diffusion coefficient of H_2O was 1.4×10^{-5} cm^2/s while the diffusion coefficient of CH_3OH was 2×10^{-5} cm^2/s, indicating that plasticization and swelling by the other component has a substantial effect on the diffusion of each component.

PUBLICATIONS

1. F. Uribe, M.S. Wilson, T.E. Springer and S. Gottesfeld, "Oxygen Reduction (ORR) at the Pt/Recast Ionomer Interface and Some General Comments on the ORR at Pt/Aqueous Electrolyte Interfaces," *Proc. of the Workshop on Structural Effects in Electrocatalysis and Oxygen Electrochemistry, D.A.* Scherson, D. Tryk, M. Daroux and X. Xing, Eds., Volume 92-11, pp.494-509 (1992).
2. M.S. Wilson and S. Gottesfeld, "Thin-Film Catalyst Layers for Polymer Electrolyte Fuel Cell Electrodes," *J. Appl. Electrochem.* **22**, 1 (1992).
3. M.S. Wilson and S. Gottesfeld, "High Performance Catalyzed Membranes Of Ultra-low Pt Loadings for Polymer Electrolyte Fuel Cells," *J. Electrochem. Soc.* **139**, L28 (1992).
4. F.A. Uribe, T.E. Springer and S. Gottesfeld, "A Microelectrode Study of Oxygen Reduction at the Platinum-Recast Nafion Film Interface," *J. Electrochem. Soc.* **139**, 765 (1992).

Electrocatalysis of Fuel Cell Reactions

J. McBreen (Brookhaven National Laboratory)

The purpose of this work is to increase the understanding of electrocatalysis on a molecular level and to apply this knowledge to fuel cells. The goals of this project are to reduce the Pt requirements for PEMFC, and to develop non-Pt catalysts for oxygen reduction and catalysts for the direct oxidation of methanol. Work in 1992 included extended X-ray absorption (XAS) studies of carbon supported Pt alloy catalysts.

EXAFS studies of Pt alloy catalysts: In situ XAS measurements were completed on carbon supported Pt/Cr, Pt/Co and Pt/Ni alloy catalysts from ETEK Corporation (ETEK) and Johnson Matthey (JM). Results were also obtained on a Pt/Mn catalyst from JM. Studies were undertaken to correlate the electrocatalytic activity of these alloy catalysts for oxygen reduction with the d-band occupancy determined from the XAS measurements. The ETEK catalysts are made by carbothermic reduction of the alloying element and heat treatment at 900°C. Measurements of the step height for the absorption of the alloying element indicated that the JM catalysts contained a higher percentage of the alloying element. The alloying procedure used by JM is proprietary but the XAS results indicate that a higher alloying temperature may have been used.

Electrodes were prepared from the alloy catalysts, vitreous carbon fibers (15%) and PTFE (12%) using a vacuum table paper-making technique. Metal oxides of the alloying element were removed by soaking the electrodes in either acid (Pt/Co and Pt/Ni) or alkaline (Pt/Cr) solutions. The electrodes were incorporated into spectroelectrochemical cells that contained 1 M $HClO_4$ electrolyte. XAS measurements were made at the K edges of the respective first row transition metal and at the L_2 and L_3 Pt edges. Measurements at both the Pt L_2 and L_3 edges permit calculation of the d-character of the catalyst. In the preliminary data analysis, the results were compared at 0.3 V (*vs.* SCE). A summary of the results are presented in Table 1. Alloying Pt with Co and Ni increases the density of the unoccupied Pt d-states, with Ni having the larger effect. The effects are more pronounced in the JM alloys. The concentration of the alloying component is higher in these alloys. Chromium has a smaller effect and Mn almost no effect. There appears to be a good correlation between the d-band vacancies and the Pt-Pt bond length; with an increase in the d-band vacancies resulting in a decrease in the Pt-Pt bond length. XANES data at the Ni edge indicated a Ni redox reaction for the ETEK catalyst but none for the JM catalyst.

Figure 24 shows the polarization curves for oxygen reduction on these catalysts in a PEMFC. It appears that any perturbation of the Pt d-character and Pt-Pt bond length is beneficial. The enhanced catalysis by the Pt/Ni catalyst (ETEK) can be attributed to a redox process involving Ni.

LAWRENCE BERKELEY LABORATORY
UNIVERSITY OF CALIFORNIA
TECHNICAL INFORMATION DEPARTMENT
BERKELEY, CALIFORNIA 94720